Landau theory of the martensitic transition in A-15 compounds*

R. N. Bhatt and W. L. McMillan
Department of Physics, and Materials Research Laboratory, University of Illinois at Urbana-Champaign, Urbana, Illinois 61801

(Received 1 March 1976)

Based on Gorkov's physical model of a Peierls-like charge-density-wave-driven transition, a Landau theory has been formulated for the structural phase transition in the A-15 compounds. Pretransition elastic anomalies, softening of the [110] transverse ([1$\bar{1}$0] polarized) phonon, sublattice distortions, variation of transition temperature with stress, and alloying and other effects have been accurately predicted, and a detailed comparison is made with experimental results. Central peaks in neutron scattering are shown to be nondynamic in nature and no pretransition forbidden (300) reflection is predicted. The Γ_{12} optic mode does not go soft at the transition, though its frequency is expected to be temperature dependent right up to room temperature.

I. INTRODUCTION

The A-15 compounds have been of great interest since 1954 when it was found that these compounds became superconductors at relatively high temperatures—V_3Si at 17 °K and Nb_3Sn at 18 °K. Since then, the superconducting properties of a wide variety of these compounds and pseudobinary alloys have been studied in a search for materials for high-field magnets and electrical power applications.

The A-15 crystal structure is shown in Fig. 1. Subsequent to the discovery of their high superconducting temperatures, structural instabilities were observed in many A-15 compounds. For V_3Si, Batterman and Barrett[1] found a (martensitic) transition from the cubic A-15 structure above 21 °K to a tetragonal structure with $c/a \simeq 1.002$ at low temperature. Testardi *et al.*[2] found that the elastic constant $(C_{11}-C_{12})$ softens with decreasing temperature and approaches zero at the martensitic transition temperature. Similar behavior is found in Nb_3Sn.

Shirane and Axe[3a] have determined the symmetry and atomic positions of the tetragonal phase of Nb_3Sn. As shown in Fig. 2, there is a flattening of the unit cell (tetragonal distortion), and a pairing of transition metal atoms in two of the linear chains. Shirane, Axe, and co-workers[3a,3b] have also measured the phonon frequency (versus wavenumber and temperature) for the [110] phonon with transverse polarization [1$\bar{1}$0], which shows considerable softening right up to the zone boundary. Several other A-15 compounds and pseudobinaries are known to exhibit martensitic transformations or the precursor elastic softening; only Nb_3Sn and V_3Si have been extensively studied. Several excellent review articles exist on the martensitic transition and the superconducting properties of the A-15's.[4-7]

Since the suggestion by Anderson and Blount[8] that the structural transition is due to some hidden order parameter, theories to date have exploited the quasi-one-dimensional electronic band structure of the linear orthogonal chains of transition metals in the A-15 compounds to explain the transition as electronically driven,[9-11,16] though soft optic modes[12] and the role of vacancies[13] have also been proposed.

The first microscopic model of the martensitic transition, due to Labbe and Friedel,[9] assumes a one-dimensional band structure for each linear chain with no interchain coupling. The Fermi energy is placed close to the bottom of one of the empty d bands (the point Γ in reciprocal space), where there is a singular behavior of the one-dimensional (1D) density of states $[n(E) \sim E^{-1/2}]$.

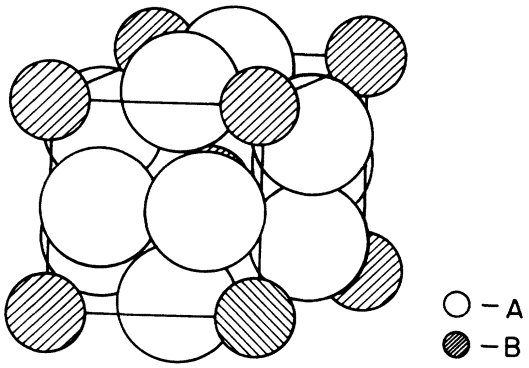

FIG. 1. A-15 structure, A_3B. (Nontransition) atoms B form a bcc lattice, and the (transition metal) atoms A form three orthogonal chains along the cube faces.

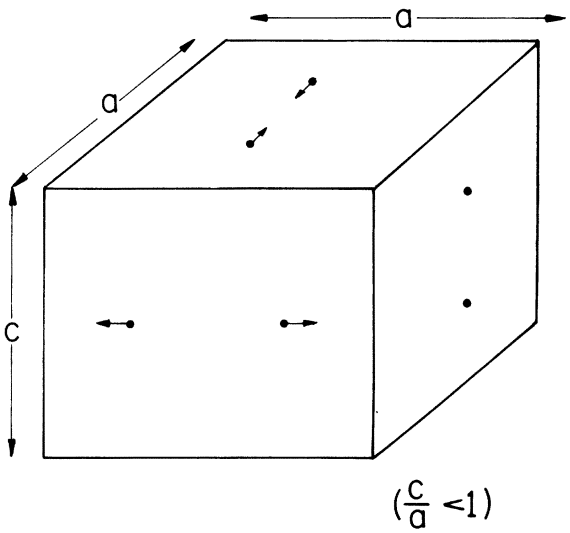

FIG. 2. Tetragonal phase in Nb_3Sn ($c/a<1$). Cell deformation is accompanied by a $\Gamma_{12}(+)$ sublattice distortion.

The transition is regarded as a second-order Jahn-Teller effect, where the degeneracy of the 1D bands is broken by the tetragonal distortion. Subsequently, it was shown[10] that the essential point of the Labbe-Friedel model is a sharp variation of the density of states near the Fermi surface. By adjusting the position of the Fermi level, reasonable agreement is possible with experiment; however, Mattheiss's[14] augmented-plane-wave–linear-combination-of-atomic-orbitals (APW-LCAO) band-structure calculations show that interchain couplings have effects of the order of 1 eV, which would wipe out any one-dimensional character of the bands.

Gorkov[11] has noted that there is a degeneracy in the A-15 band structure at the X point (at the center of the zone face of the simple cubic Brillouin zone) in the cubic phase which is lifted by pairing of the transition-metal atoms in the tetragonal phase. The energy gap at the X point is proportional to the amplitude of the optic-phonon mode which pairs the transition-metal atoms. If this portion of the band structure lies near the Fermi energy, the electronic energy will be lowered as the energy gap opens up. Thus Gorkov's model of the martensitic transition is analogous to the Peierls transition in one-dimensional metals and closely related to the charge-density-wave transitions in the transition-metal dichalcogenides.

The Peierls transition refers to the instability of a one-dimensional metallic (odd number of electrons per atom) chain to a displacement of wave-vector π/d, where d is the spacing of atoms, in the presence of a small electron-phonon interaction. This causes the neighboring atoms to pair up, and a gap Δ opens up at the Fermi surface ($k=\pi/2d$), resulting in a lowering of the electronic energy. The size of the gap is proportional to the atomic displacements, and the equilibrium displacement at $T=0$ is given by minimizing the total energy, which is made up of the lattice part (proportional to Δ^2) and the electronic part {which is reduced by an amount $(\Delta^2/4E_F)\,[\frac{1}{2}+\ln(4E_F/\Delta)]$ by the opening of the gap at the Fermi surface}. The decrease in total energy at the minimum is equal to the square of the gap multiplied by the density of states of electrons of one spin at the Fermi surface.

Such a transition is conceivable in the case of weakly interacting 1D chains in a three-dimensional (3D) lattice. Furthermore, while a correct treatment of fluctuations in 1D systems shows that a transition is only possible at zero temperature, finite transition temperatures are possible in the case of the quasi-one-dimensional chains in the 3D lattice, and a Landau-like mean-field theory can work. This is the kind of picture that Gorkov envisages for the structural transformation in the A-15 compounds—a Peierls-like electronically driven transition of the linear chains of transition-metal atoms in the A-15 structure which causes a tetragonal deformation of the crystal (to which the electron charge density is coupled via the Γ_{12} optic phonon).

Gorkov starts[11a] with a model of three noninteracting chains, in which case if the conduction band is well separated from the s and p bands, then the Fermi surface will pass through the midpoints X of the faces of the cubic Brillouin zone, where the bands are double degenerate with a finite slope. If overlap of different strings is taken into account, perturbatively, the resulting spectrum is shown[11b] to have a logarithmic divergence of the density of states at the X-point energy, and therefore locating of the Fermi surface near the X point could account for the high density of states needed to explain the properties of the A-15's. The elastic constants are found to have a $\ln T$ behavior, as does the magnetic susceptibility. The structural instability and superconductivity, both due to the instability of the electron spectrum, are intimately related in this model (as for the Peierls chain) and the transition temperatures are predicted to be of the same order of magnitude.

We believe that Gorkov's physical picture of the martensitic transition is correct, and our Landau theory is based on it. Unfortunately, Gorkov's microscopic calculations use a one-dimensional band structure, and can therefore not be applied in their present form to the A-15 compounds. Our Landau theory is free of this assumption of a one-

dimensional band structrue; it therefore allows us to test the model of an electronically driven charge-density-wave transition without making inappropriate assumptions about the band structure.

The present Landau theory follows along the lines of the theory developed for the charge density waves in the transition-metal dichalcogenides.[15] The transition-metal d-band electron charge density is coupled to the optic modes which pair the transition-metal atoms, which in turn are coupled to the dilatations of the lattice by a coupling analogous to the one first included in Sham's lattice-dynamical model.[16] The theory predicts the softening of the elastic constant $(C_{11}-C_{12})$ while the bulk modulus $(C_{11}+2C_{12})$ and shear modulus C_{44} are temperature independent in this approximation. (Gorkov has shown that the variation of C_{44} can be explained in terms of interchain electronic couplings, which we have left out of our model.) The higher-order terms explain the pressure, uniaxial stress, and composition dependence of the tetragonality. In order to study the behavior of the phonon modes at finite wave vector, a dynamical Landau theory is formulated treating the electron charge density and lattice displacement as independent dynamical variables. The equations of motion in the cubic phase are solved and the dynamic structure factor calculated for the (110) phonon with transverse $(1\bar{1}0)$ polarization. The predicted k dependence of the frequency is in good agreement with the neutron scattering data.[3] The central peak is shown to be nondynamic, and the predicted temperature dependence of a static impurity peak is in good agreement with experiment. For the values of the parameters appropriate for the A-15 compounds, no optic mode is found to go soft, though a reduction in frequency near the transition is indicated. An extensive comparison of theory with the experimental results is done in Sec. VII after the theoretical details (Secs. II–VI), and the relation with superconductivity is discussed in Sec. VIII.

II. LANDAU THEORY

The central point of a Landau theory is an expansion of the free energy in powers of the order parameter and its gradients. The order parameter in the present case is the d-band electron charge density; in the A-15 structure there are three possible charge density waves [with wave vectors $(2\pi/a,0,0)$, $(0,2\pi/a,0)$ and $(0,0,2\pi/a)$] which open up an energy gap at the three X points. These three charge-density waves (CDW's) are coupled, respectively, to the optical phonons which pair the transition-metal atoms in the linear chains running in the x, y, and z directions. The optical phonons are coupled bilinearly to dilatations of the unit cell giving nine coupled modes. Each CDW is locked into the lattice and its phase is fixed with respect to the lattice. The CDW peaks between the transition metals which are paired form a bond charge. Thus only the amplitude of the CDW can vary and one represents the CDW's by real order parameters $\phi_\mu(\vec{r})$ where $\mu=x,y,z$. (Throughout this paper we will use greek indices to represent x, y, and z and roman indices to represent 1, 2, 3. Further, since quantities with subscripts will not necessarily refer to a component of a tensor, repeated induces will *not* be summed over except where the summation is explicitly shown.) For definiteness, in the static theory, one can choose ϕ_x to be the amplitude of the $(2\pi/a,0,0)$ Fourier component of the charge density. In the dynamic theory, we choose to factor out the $\vec{k}=(2\pi/a,0,0)$ variation from $\phi_x(\vec{r})$, which thus contains only long-wavelength variations. For purposes of comparing the Landau theory with the microscopic theory and with measurements of the band gap, it is more convenient to write the free energy in terms of the magnitude of the energy gap $v_\mu(\vec{r})$, rather than $\phi_\mu(\vec{r})$. In the static theory near the phase transition, the two are simply proportional to each other so that one has a choice of which to use as an order parameter. In the dynamic theory, however, $v_\mu(\vec{r})$ adiabatically follows the optical-phonon amplitude, whereas $\phi_\mu(\vec{r})$ is determined by the electron distribution function which has a characteristic relaxation time; in order to present this relaxation process correctly, one must use $\phi_\mu(\vec{r})$ as the order parameter. So as to cause least confusion, therefore, we use the CDW amplitude as the order parameter throughout; the magnitude of the gap is used only in Secs. VII D and VII G.

We choose the following form for the electronic free energy:

$$F_1=\frac{1}{2}\int d^3r\sum_\mu\{a_\mu\phi_\mu^2(\vec{r})+b\,\phi_\mu^4(\vec{r})+c_1[\partial_\mu\phi_\mu(\vec{r})]^2+c_2[\vec{\nabla}\phi_\mu(\vec{r})]^2+u_\mu(\vec{r})\,\phi_\mu(\vec{r})\}. \quad (1)$$

$u_\mu(\vec{r})$ represents the coupling to an external potential or an impurity potential. The parameter a_μ is approximately linear in temperature near the transition temperature

$$a_\mu=a'(T-T_{mo}^{\mu}), \quad (2)$$

while the other parameters are temperature independent. The gain in electronic energy is the greatest (and the martensitic transition temperature the highest) when the Fermi energy lies approximately at the X-point energy $E_{X\mu}$. Expanding

about that maximum, we have

$$T_{m\,o}^{\mu} = T_m^{\max} - B(E_F - E_{X\mu})^2 . \tag{3}$$

The X-point energy is shifted by the lattice stain $\epsilon_{\mu\nu}$ and we can write

$$E_{X\mu} = E_X^0 + \lambda_1 \epsilon_{\mu\mu} + \lambda_2 \sum_{\nu} \epsilon_{\nu\nu} , \tag{4}$$

so that

$$a_\mu = a'(T - T_m^0) + \Lambda_1 \epsilon_{\mu\mu} + \Lambda_2 \sum_{\nu} \epsilon_{\nu\nu} , \tag{5}$$

where

$$T_m^0 = T_m^{\max} - B(E_F - E_X^0)^2 , \tag{6a}$$

$$\Lambda_1 = 2B\lambda_1 (E_F - E_X^0) , \tag{6b}$$

$$\Lambda_2 = 2B\lambda_2 (E_F - E_X^0) . \tag{6c}$$

Note that both Λ_1 and Λ_2 change sign as the Fermi level passes through E_X^0 and the martensitic transition temperature goes through its maximum. The sign of the tetragonal distortion $(c/a - 1)$ is determined by the sign of Λ_1 and the pressure dependence of T_m is controlled by Λ_2.

In order to determine the coupling of the charge density to the phonons, we consider the displacements of the transition-metal atoms in the presence of strain. The positions of the transition-metal atoms in the [100] chain can be written

$$\vec{R}_1 = [\tfrac{1}{4}\vec{x} + \hat{x}\, Q_x(\vec{R}_1^0)] + \tfrac{1}{2}\vec{z} , \tag{7a}$$

$$\vec{R}_2 = [\tfrac{3}{4}\vec{x} - \hat{x}\, Q_x(\vec{R}_2^0)] + \tfrac{1}{2}\vec{z} , \tag{7b}$$

where $\vec{x}$, $\vec{y}$, and $\vec{z}$ are the translation vectors of the strained unit cell and $Q_x(\vec{r})$ defines the optic-mode amplitude at the position of the unit cell in question. It corresponds to the pairing up of the atoms along the (100) chain for the wave vector $\vec{k} = (2\pi/a, 0, 0)$.

With similar definitions for $Q_y(\vec{r})$ and $Q_z(\vec{r})$, the electron phonon coupling term becomes

$$F_2 = \int d^3r f \sum_{\mu} Q_\mu(\vec{r})\, \phi_\mu(\vec{r}) . \tag{8}$$

Finally, the elastic free energy (in the harmonic approximation) may be written in terms of the strain tensor $\epsilon_{\mu\nu}$ and the optic-mode amplitudes $Q_\mu(\vec{r})$

$$F_3 = \frac{1}{2}\int d^3r \left(\sum_{\mu} K_{11}\epsilon_{\mu\mu}^2 + \sum_{\mu\neq\nu} (2K_{44}\epsilon_{\mu\nu}\epsilon_{\mu\nu} + K_{12}\epsilon_{\mu\mu}\epsilon_{\nu\nu}) + \sum_{\mu} (K_0 + G)Q_\mu^2 + G\sum_{\mu\neq\nu} Q_\mu Q_\nu \right.$$
$$\left. + 2h[\epsilon_{xx}(Q_y - Q_z) + \epsilon_{yy}(Q_z Q_x) + \epsilon_{zz}(Q_x - Q_y)] - 2\sum \zeta_\mu \epsilon_{\mu\mu} \right) . \tag{9}$$

The terms involving ζ_μ represent coupling to external stresses and permit calculation of the elastic constants. Couplings of the off-diagonal components of the strain tensor with external stresses have been left out, as these variables will turn out to be irrelevant in the present theory within the quadratic approximation.

The elastic constants K_{11}, K_{12}, and K_{44} are the unrenormalized values of the conventional constants C_{11}, C_{12}, and C_{44}, respectively.

At this stage it should be pointed out that only the three relevant optic modes and the acoustic modes (described by the strain tensor) have been included in the free energy; the other 18 phonon modes have been omitted.

The usual Landau-theory restrictions apply. The theory is valid only near the transition temperature and predicts correct temperature dependences only when critical fluctuations are unimportant. The order parameters are assumed to vary smoothly in space with wavelengths much larger than the lattice spacing. In addition, because of the complexity of the model, many terms which are permitted by symmetry have been omitted. For example, the phonon free energy is assumed to be harmonic and only anharmonic terms appear in the electronic free energy. Similarly, only the k variation of the electronic free energy has been retained; the optic modes have been assumed to be k independent, while the acoustic modes are assumed to have frequencies varying linearly with wave vector. (The latter seems to be valid almost halfway to the zone boundary.) We believe that the omitted terms are unimportant, but one should keep in mind that not all terms permitted by symmetry have been retained. This completes the static Landau theory.

The dynamic Landau theory follows along the lines of the dynamic theory for the transition-metal dichalcogenides.[15b] In the dynamic calculation, it is convenient to work with the amplitudes of the acoustic modes $\delta_\mu(\vec{r})$ rather than the strain tensor $\epsilon_{\mu\nu}(\vec{r})$. The strain tensor and the acoustic-mode amplitudes are related by $\epsilon_{\mu\nu} = \frac{1}{2}(\partial_\mu \delta_\nu + \partial_\nu \delta_\mu)$, and that permits us to write the free energy in terms of δ_μ. In addition, to do dynamics, we require the lattice kinetic energy

$$K = \frac{1}{2}\int d^3r \left(m\sum_{\mu} [\dot{\delta}_\mu(\vec{r})]^2 + M\sum_{\mu} [\dot{Q}_\mu(\vec{r})]^2 \right) , \tag{10}$$

where m and M are the mass densities associated with the acoustic and optic modes, respectively, and the dot indicates a time derivative. The dissipative terms associated with the charge-density wave are expressed in terms of the dissipation function

$$D = \int d^3r \gamma \sum_\mu \left(\frac{\partial \phi_\mu}{\partial t}\right)^2 . \tag{11}$$

To compute the dynamic structure factor, we need to consider the system in equilibrium with a thermal reservoir, which pumps power lost by the system because of the dissipative term back into the system via a random thermal force. Such a process may be represented by the term

$$R = \int d^3r \sum_\mu g_\mu \left(\frac{\partial \phi_\mu}{\partial t}\right), \tag{12}$$

where $g_\mu(\vec{r}, t)$ is a Gaussian-distributed random function with a correlation function

$$\langle g_\mu(\vec{r}, t) g_\nu(\vec{r}', t')\rangle = \gamma k T \delta_{\mu\nu} \delta(\vec{r} - \vec{r}') \delta(t - t') . \tag{13}$$

The dynamical equations are just the generalized Lagrangian equations of motion. It is convenient to Fourier transform the space dependence of the variables; after doing so, the equations of motion become

$$0 = -\frac{\partial F}{\partial \phi_{\mu q}} - \frac{1}{2}\frac{\partial D}{\partial \dot{\phi}_{\mu q}} + \frac{\partial R}{\partial \dot{\phi}_{\mu q}}, \tag{14a}$$

$$\frac{d}{dt}\frac{\partial K}{\partial \dot{\delta}_{\mu q}} = -\frac{\partial F}{\partial \delta_{\mu q}}, \tag{14b}$$

$$\frac{d}{dt}\frac{\partial K}{\partial \dot{Q}_{\mu q}} = -\frac{\partial F}{\partial Q_{\mu q}} . \tag{14c}$$

III. STATIC THEORY IN THE QUADRATIC APPROXIMATION

We consider first the quadratic part of the free energy in the absence of external stresses in the uniform limit

$$\frac{F_0}{V} = \frac{1}{2}\sum_\mu [a\phi_\mu^2 + K_{11}\epsilon_{\mu\mu}^2 + (K_0 + G)Q_\mu^2 + 2fQ_\mu\phi_\mu]$$
$$+ \sum_{\mu\neq\nu} (2K_{44}\epsilon_{\mu\nu}\epsilon_{\mu\nu} + K_{12}\epsilon_{\mu\mu}\epsilon_{\nu\nu} + GQ_\mu Q_\nu)$$
$$+ 2h[\epsilon_{\mu\mu}(Q_y - Q_z) + \text{permutations}], \tag{15}$$

where $a = a'(T - T_m^0)$ in this approximation. In the above expression, the off-diagonal components of the strain tensor (ϵ_{xy}, ϵ_{yz}, and ϵ_{zx}) do not couple with anything, and therefore do not take part in the transition. Hence they will be omitted from consideration until we discuss the dynamical problem.

In order to put the free energy into a block diagonal form, we define the linear combinations

$$\epsilon_1 = (\epsilon_{xx} + \epsilon_{yy} + \epsilon_{zz})/\sqrt{3}, \tag{16a}$$

$$\epsilon_2 = (\epsilon_{xx} - \epsilon_{yy})/\sqrt{2}, \tag{16b}$$

$$\epsilon_3 = (\epsilon_{xx} + \epsilon_{yy} - 2\epsilon_{zz})/\sqrt{6} \tag{16c}$$

and similarly ϕ_i and Q_i in terms of the ϕ_μ and Q_μ.

In terms of the new variables the free energy becomes

$$F = \frac{1}{2}\sum_{j=1}^{3} \tilde{V}_j M_j V_j, \tag{17}$$

where V_j are the three-component "vectors"

$$V_1 = \begin{pmatrix} \phi_1 \\ Q_1 \\ \epsilon_1 \end{pmatrix}, \quad V_2 = \begin{pmatrix} \phi_2 \\ Q_2 \\ \epsilon_3 \end{pmatrix}, \quad V_3 = \begin{pmatrix} \phi_3 \\ Q_3 \\ \epsilon_2 \end{pmatrix}; \tag{18}$$

and M_j are the 3×3 matrices

$$M_1 = \begin{pmatrix} a & f & 0 \\ f & K_0 + 3G & 0 \\ 0 & 0 & K_{11} + 2K_{12} \end{pmatrix}, \tag{19a}$$

$$M_2 = \begin{pmatrix} a & f & 0 \\ f & K_0 & -\sqrt{3}\,h \\ 0 & -\sqrt{3}\,h & K_{11} - K_{12} \end{pmatrix}, \tag{19b}$$

$$M_3 = \begin{pmatrix} a & f & 0 \\ f & K_0 & \sqrt{3}\,h \\ 0 & \sqrt{3}\,h & K_{11} - K_{12} \end{pmatrix} . \tag{19c}$$

Thus, the modes break up into groups which are decoupled from one another. The transition temperatures corresponding to the three modes (originally ϕ_i) are modified to different extents by the electron-phonon coupling. The transition temperatures are obtained by determining the temperatures at which one of the eigenvalues of the M_j matrices is zero. It is straightforward to show that the transition temperatures corresponding to the three cases and the eigenvectors corresponding to the zero eigenvalues are given by

$$T_1 = T_m^0 + f^2/(K_0 + 3G)a', \tag{20a}$$

$$T_2 = T_3 = T_m^0 + \frac{f^2/K_0 a'}{1 - 3h^2/K_0(K_{11} - K_{12})} = T_m^*, \tag{20b}$$

with eigenvectors (unnormalized):

$$e_1=\begin{pmatrix}1\\ \dfrac{-f}{K_0+3G}\\ 0\end{pmatrix};\quad e_2=\begin{bmatrix}1\\ \dfrac{-f}{K_0-3h^2/(K_{11}-K_{12})}\\ \dfrac{-\sqrt{3}\,hf}{K_0(K_{11}-K_{12})-3h^2}\end{bmatrix};$$

$$e_3=\begin{bmatrix}1\\ \dfrac{-f}{K_0-3h^2/(K_{11}-K_{12})}\\ \dfrac{\sqrt{3}\,hf}{K_0(K_{11}-K_{12})-3h^2}\end{bmatrix}. \tag{21}$$

From Eq. (20) it follows that unless G is large and negative $[G<-3h^2/(K_{11}-K_{12})]$, the latter two modes, which involve distortions of the unit cell, have higher-transition temperatures, and are therefore picked by nature. {In the other case, [i.e., $G<-3h^2/(K_{11}-K_{12})$], the theory predicts a Peierls-type pairing up of the transition-metal atoms in each of the three orthogonal chains without any change in the unit cell; this case is clearly not identifiable with the A-15 martensitic transition, so we shall not discuss it any further.}

The quadratic theory thus predicts a transition at a temperature T_m^* involving either a tetragonal or an orthorhombic distortion of the lattice, but cannot select either over the other. We shall have to consider the effects of cubic terms to determine which type of distortion actually occurs in the crystal.

From Eq. (20b), the renormalized parameter $a_r=a'(T-T_m^*)$ is related to its unrenormalized value $a=a'(T-T_m^0)$ by

$$a_r=a-\frac{f^2/K_0}{1-3h^2/K_0(K_{11}-K_{12})}. \tag{22}$$

In order to calculate the elastic constants as a function of temperature, we must include the terms involving coupling to the external stresses. However, from the fact that off-diagonal components of the stress tensor and its trace $\sum_\mu \epsilon_{\mu\mu}$ decouple from the other modes, it follows immediately that the bulk modulus $\frac{1}{3}(K_{11}+2K_{12})$ and shear modulus K_{44} are not renormalized and are therefore independent of temperature

$$C_{11}(T)+2C_{12}(T)=K_{11}+2K_{12}, \tag{23a}$$

$$C_{44}(T)=K_{44}. \tag{23b}$$

To get the temperature variation of the other linear combination, $(C_{11}-C_{12})$, we consider the relevant portion of the free energy

$$\mathfrak{F}=\tfrac{1}{2}[a\phi_2^2+K_0Q_2^2+2f\phi_2Q_2+(K_{11}-K_{12})\epsilon_3^2 - 2\sqrt{3}\,hQ_2\epsilon_3-2\zeta_3\epsilon_3],$$

where $\zeta_3=(\zeta_x+\zeta_y-2\zeta_z)/\sqrt{6}$. By minimizing the free energy with respect to ϕ_2, Q_2, and ϵ_3 for a given ζ_3, we get a set of linear equations which may be used to get ϵ_3 as a function of ζ_3

$$\epsilon_3=\frac{\zeta_3}{K_{11}-K_{12}-3h^2/(K_0-f^2/a)},$$

from which the elastic constant $(C_{11}-C_{12})$ is easily obtained

$$C_{11}(T)-C_{12}(T)=\frac{\partial\zeta_3}{\partial\epsilon_3}=K_{11}-K_{12}-\frac{3h^2}{K_0} - \frac{3h^2f^2}{K_0^2}\Big/\left(a_r+\frac{3h^2f^2/K_0^2}{K_{11}-K_{12}-3h^2/K_0}\right), \tag{23c}$$

where we have expressed a in terms of the renormalized parameter a_r. Far from the transition $a_r\to\infty$ and thus Eq. (23c) gives the limiting high-temperature value of the elastic constant as

$$C_{11}-C_{12}=K_{11}-K_{12}-3h^2/K_0. \tag{24}$$

(We shall use the convention that C_{ij} without any argument refers to the renormalized high-temperature value.) In terms of the renormalized quantity $(C_{11}-C_{12})$, Eqs. (22) and (23c) become

$$a_r=a-\frac{f^2}{K_0}-\frac{3h^2f^2/K_0^2}{C_{11}-C_{12}} \tag{25}$$

$$C_{11}(T)-C_{12}(T)=(C_{11}-C_{12})\times\left[1-\left(1+\frac{K_0^2a_r(C_{11}-C_{12})}{3h^2f^2}\right)^{-1}\right] =(C_{11}-C_{12})[1-(1+\beta\theta)^{-1}], \tag{26}$$

where

$$\theta=(T-T_m^*)/T_m^* \tag{27}$$

is the reduced temperature and

$$\beta=(C_{11}-C_{12})(K_0^2a'T_m^*/3h^2f^2) \tag{28}$$

is a dimensionless inverse coupling parameter.

Thus the static theory in the quadratic approximation predicts a tetragonal or orthorhombic distortion of the unit cell at the (renormalized) transition temperature T_m^*. Furthermore, it predicts only a softening of the linear combination $[C_{11}(T)-C_{12}(T)]$ of elastic constants, which goes to zero at T_m^*; the other linear combinations $[C_{11}(T)+2C_{12}(T)]$ and $C_{44}(T)$ are predicted to be independent of temperature near the transition.

IV. STATIC THEORY—II: HIGHER-ORDER TERMS

In order to consider the nature and order of the actual phase transition in the A-15 structure, we consider the full expression for the free energy in the absence of stresses in the uniform limit

$$F=\frac{V}{2}\Big(\sum_{\mu}[a_{\mu}\phi_{\mu}^{2}+b\phi_{\mu}^{4}+K_{11}\epsilon_{\mu\mu}^{2}+(K_{0}+G)Q_{\mu}^{2}+2fQ_{\mu}\phi_{\mu}]$$
$$+\sum_{\mu\neq\nu}(2K_{44}\epsilon_{\mu\nu}+K_{12}\epsilon_{\mu\mu}\epsilon_{\nu\nu}+GQ_{\mu}Q_{\nu})$$
$$+2h[\epsilon_{xx}(Q_{y}-Q_{z})+\text{permutations}]\Big), \tag{29}$$

where

$$a_{\mu}=a+\Lambda_{1}\epsilon_{\mu\mu}+\Lambda_{2}\sum_{\nu}\epsilon_{\nu\nu}. \tag{30}$$

Near the phase transition, the quadratic theory showed that only the linear combinations e_2 and e_3 defined in Eq. (21), whose eigenvalues go to zero at the "Gaussian" transition temperature T_m^*, are relevant. We first express Eq. (29) in terms of the ϕ_i, Q_i, and ϵ_i. Putting the irrelevant variables ϕ_1, Q_1, and ϵ_1 to zero, we have

$$F=\tfrac{1}{2}V\{a(\phi_{2}^{2}+\phi_{3}^{2})+\tfrac{1}{2}b(\phi_{2}^{2}+\phi_{3}^{2})^{2}$$
$$+\tfrac{1}{6}\Lambda_{1}[\epsilon_{3}(\phi_{2}^{2}-\phi_{3}^{2})+2\epsilon_{2}\phi_{2}\phi_{3}]$$
$$+K_{0}(Q_{2}^{2}+Q_{3}^{2})+2f(\phi_{2}Q_{2}+\phi_{3}Q_{3})$$
$$+(K_{11}-K_{12})(\epsilon_{2}^{2}+\epsilon_{3}^{2})+2\sqrt{3}\,h(\epsilon_{2}Q_{3}-\epsilon_{3}Q_{2})\}. \tag{31}$$

Near T_m^*, according to the above discussion, only e_2 and e_3 need be considered. Consequently, from Eq. (21),

$$\phi_{2}=-\frac{K_{0}(C_{11}-C_{12})}{\sqrt{3}\,hf}\epsilon_{3},\quad Q_{2}=\left(\frac{C_{11}-C_{12}}{\sqrt{3}\,h}+\frac{\sqrt{3}\,h}{K_{0}}\right)\epsilon_{3},$$
$$\phi_{3}=\frac{K_{0}(C_{11}-C_{12})}{\sqrt{3}\,hf}\epsilon_{2},\quad Q_{3}=-\left(\frac{C_{11}-C_{12}}{\sqrt{3}\,h}+\frac{\sqrt{3}\,h}{K_{0}}\right)\epsilon_{2},$$

so that Eq. (31) becomes

$$F/V=\alpha_{2}(\epsilon_{2}^{2}+\epsilon_{3}^{2})+\alpha_{3}\epsilon_{3}(\epsilon_{3}^{2}-3\epsilon_{2}^{2})+\alpha_{4}(\epsilon_{2}^{2}+\epsilon_{3}^{2})^{2}, \tag{32}$$

where

$$\alpha_{2}=\alpha_{2}'(T-T_{m}^{*})=\tfrac{1}{2}a_{r}[K_{0}^{2}(C_{11}-C_{12})^{2}/3h^{2}f^{2}], \tag{33a}$$
$$\alpha_{3}=(\Lambda_{1}/2\sqrt{6})[K_{0}^{2}(C_{11}-C_{12})^{2}/3h^{2}f^{2}], \tag{33b}$$
$$\alpha_{4}=\tfrac{1}{4}b[K_{0}^{4}(C_{11}-C_{12})^{4}/9h^{4}f^{4}]. \tag{33c}$$

Minimizing Eq. (32) with respect to ϵ_2 and ϵ_3 we get that for $\alpha_3\neq 0$, $\epsilon_3=0$ implies $\epsilon_2=0$, i.e., it is not possible to have an orthorhombic distortion without the tetragonal one. In fact, the minima for nonzero distortions correspond to $\epsilon_2=0$ and $\epsilon_2=\pm\sqrt{3}\,\epsilon_3$, which are all tetragonal distortions corresponding to the tetragonal axis along z, x, and y, all three of which should be possible on the basis of symmetry. Thus we see that the cubic terms help decide in favor of the mode involving a tetragonal distortion, along with a sublattice distortion of the type $Q_2\sim(Q_x-Q_y)$. The tetragonal axis may be along any one of the x, y, and z directions, and for the rest of this discussion, we chose it to lie along the z axis, i.e., $\epsilon_2=0$. With this, Eq. (32) reads

$$F/V=\alpha_{2}\epsilon_{3}^{2}+\alpha_{3}\epsilon_{3}^{3}+\alpha_{4}\epsilon_{3}^{4}. \tag{34}$$

A free energy of the type [Eq. (34)] describes a first-order transition at a temperature given by

$$T_{m}=T_{m}^{*}+\alpha_{3}^{2}/4\alpha_{2}'\alpha_{4}. \tag{35}$$

Below T_m, the distortion is given by

$$\epsilon_{3}=-\frac{3\alpha_{3}}{8\alpha_{4}}\left[1+\left(1-\frac{32\alpha_{2}'\alpha_{4}(T-T_{m}^{*})}{9\alpha_{3}^{2}}\right)^{1/2}\right]$$
$$=-\frac{3\alpha_{3}}{8\alpha_{4}}\left[1+\frac{1}{3}\left(1+\frac{32\alpha_{2}'\alpha_{4}(T_{m}-T)}{\alpha_{3}^{2}}\right)^{1/2}\right]. \tag{36}$$

In particular, the distortions at the transition temperature and far below the transition are given by

$$\epsilon_{3}(T_{m})=-\alpha_{3}/2\alpha_{4}, \tag{37a}$$
$$\epsilon_{3}(T\ll T_{m})=-\operatorname{sgn}(\alpha_{3})[\alpha_{2}'(T_{m}-T)/2\alpha_{4}]^{1/2}, \tag{37b}$$

where in the latter equation we have assumed that $T_m-T\gg T_m-T_m^*$, so that the effect of the cubic term can be neglected.

The transition entropy is given by

$$\Delta S=-\left[\left(\frac{\partial F_{\min}}{\partial T}\right)_{T_{m}^{+}}-\left(\frac{\partial F_{\min}}{\partial T}\right)_{T_{m}^{-}}\right]=\frac{\alpha_{2}'\alpha_{3}^{2}}{4\alpha_{4}^{2}}. \tag{38}$$

$F_{\min}$ is the free energy at the minimum of Eq. (34).

Schematic plots of $\epsilon_3(T_m)$, $\epsilon_3(T\ll T_m)$, and ΔS as functions of the Fermi energy are given in Fig. 3. Since α_3 changes sign as the Fermi energy crosses the X-point energy, we see that the position of the Fermi energy relative to the energy at the X point essentially picks out the sign of the tetragonal distortion.

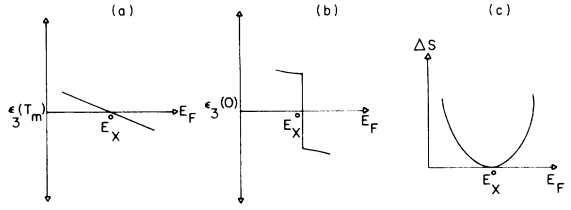

FIG. 3. Plots of tetragonal distortion at (a) and much below (b) the martensitic transition and of the entropy of the transition (c) as a function of the Fermi energy.

One more quantity of interest is the jump in specific heat at the transition. The specific heat C_v, is simply $-Td^2F_{\min}/dT^2$, and is easily shown to be

$$C_v=\begin{cases}(T\alpha_2'^2/2\alpha_4)[1+(1+32\alpha_2\alpha_4/\alpha_3^2)^{-1}], & T<T_m\\ 0, & T>T_m.\end{cases} \tag{39}$$

This is, of course, in addition to the background specific heat, which varies smoothly across the transition. A plot of C_v vs T is shown in Fig. (4). While the jump at T_m is $(2T_m\alpha_2'^2\alpha_4)$, we see that for a weakly-first-order transition, smearing of the fluctuations near T_m will cause the jump to appear to be only a quarter of that value, which is precisely the jump for a second-order transition

$$(\Delta C_v)_{T_m}^{\text{apparent}}=\frac{T_m\alpha_2'^2}{2\alpha_4}=\frac{a'^2T_m}{2b}. \tag{40}$$

Thus we see that the presence of the cubic term renders the transition first order, increases the transition temperature somewhat, and helps pick out the tetragonal phase over the orthorhombic phase, which are equally likely in the quadratic approximation. However, in view of the fact that the transverse [110] acoustic wave (polarized along the [1$\bar{1}$0] axis), which corresponds to a $(\epsilon_{xx}-\epsilon_{yy})$-type distortion, is found to go almost totally soft at the transition, and the tetragonal distortion at T_m is extremely small (at least for V_3 Si) we shall assume for the most part that the cubic terms are small, in the sense that they do not alter the transition temperature much, but just serve the purpose of picking out the nature and sign of the distortion. Accordingly, in the dynamic theory, T_m^* will be assumed to be the actual transition temperature, and fits to experimental data on ultrasonic velocity and phonon dispersion will be done accordingly.

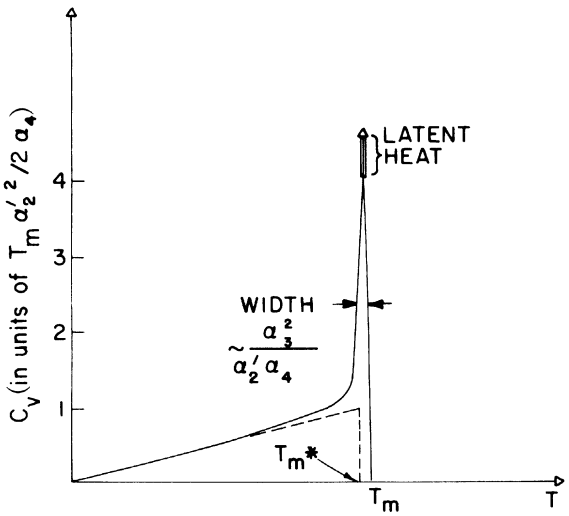

FIG. 4. Specific heat at constant volume predicted by the Landau theory for a weakly-first-order transition, along with the Landau theory result for a second-order transition (dotted line).

Next, we derive the (nonlinear) relationship between a (001) uniaxial stress and the transverse strain near the phase transition. Neglecting volume changes {since $[C_{11}(T)-C_{12}(T)]\ll[C_{11}(T)+2C_{12}(T)]$ near the phase transition}, the relevant expression for the free energy including the external stress is

$$F/V=\alpha_2\epsilon_3^2+\alpha_3\epsilon_3^3+\alpha_4\epsilon_3^4-\zeta_3\epsilon_3.$$

[We need not consider ϵ_2 as it does not couple to a (001) stress.] Minimizing F with respect to ϵ_3, we arrive at the desired expression

$$\zeta_3=2\alpha_2\epsilon_3+3\alpha_3\epsilon_3^2+4\alpha_4\epsilon_3^3, \tag{41}$$

where the α_i are defined in Eq. (33).

Before going on to the dynamical problem, we consider the effect of stress on the transition temperature. For the case of unaxial (001) stress near the phase transition, we can, as before, omit the volume change and simply add on a term $-\zeta_3\epsilon_3$ to the right-hand side of Eq. (32). If the signs of the linear and cubic terms in ϵ_3 are the same, as they are, for example, for a compressive (001) stess in a crystal of Nb_3Sn where the tetragonality is negative $(c/a<1)$, then for small stresses the transition will take place at a higher temperature and will be of the ϵ_3 type. However, for the case of V_3Si, where the tetragonality is positive, a small compressive (001) stress causes it to pick its long axis along either x or y direction. For sufficiently large stress the transition in both cases is suppressed; if the cubic term were absent, it would take an infinitesimal stress to smear out the transition and cause a smooth variation of the distortion, and thus the stress needed to wipe out the singular behavior is an estimate of the magnitude of the cubic term. The change in transition temperature caused by stresses is (as can be seen from purely dimensional considerations) of the order of $(T_m-T_m^*)$, the change in transition temperature due to the cubic term. For V_3Si, this variation has been studied[17a] and found to be no more than 0.1°, and so any fit involving the cubic term must use values consistent with this result.

The pressure dependence of the transition temperature is seen directly from Eq. (30). Since ϵ_1 does not couple to any other coordinate bilinearly, the net effect of pressure is to change the transition temperature according to

$$\frac{dT_m}{dP}=\frac{dT_m}{d\epsilon_1}\frac{d\epsilon_1}{dP}=\frac{3}{C_{11}+2C_{12}}\frac{\Lambda_2}{a'}. \tag{42}$$

Like Λ_1, Λ_2 changes sign as the Fermi surface passes through the X-point energy; consequently the sign of the pressure dependence of the transition temperature will be related to the sign of the tetragonality.

V. DYNAMICS

For studying the dynamics of the system in the high-temperature phase, the cubic and higher terms may be omitted. Further, it is convenient to work with the acoustic mode amplitudes δ_μ instead of the components of the strain tensor $[\epsilon_{\mu\nu}=\frac{1}{2}(\partial_\mu\delta_\nu+\partial_\nu\delta_\mu)]$. We write the quadratic part of the free energy in terms of the space-Fourier-transformed variables

$$F=\frac{1}{2}\sum_{\vec{k}}\Bigg(\sum_{\mu}\{(a+c_1k_\mu^2+c_2k^2)|\phi_{\mu\vec{k}}|^2+(K_0+G)|Q_{\mu\vec{k}}|^2+f(\phi_{\mu\vec{k}}^*Q_{\mu\vec{k}}+Q_{\mu\vec{k}}^*\phi_{\mu\vec{k}})+[(K_{11}-K_{44})k_\mu^2+K_{44}k^2]|\delta_{\mu\vec{k}}|^2\}$$
$$+\sum_{\mu\neq\nu}[(K_{11}+K_{44})k_\mu k_\nu\delta_{\mu\vec{k}}^*\delta_{\nu\vec{k}}+GQ_{\mu\vec{k}}^*Q_{\nu\vec{k}}]+\{ih[k_x\delta_{x\vec{k}}^*(Q_{y\vec{k}}-Q_{z\vec{k}})+k_y\delta_{y\vec{k}}^*(Q_{z\vec{k}}-Q_{x\vec{k}})+k_z\delta_{z\vec{k}}^*(Q_{x\vec{k}}-Q_{y\vec{k}})]+\text{c.c.}\}\Bigg). \tag{43}$$

Expressions for the kinetic energy, the dissipation, and the thermal force terms follow directly from Eqs. (10)–(12)

$$K=\frac{1}{2}\sum_{\vec{k}}\sum_{\mu}(M|\dot{Q}_{\mu\vec{k}}|^2+m|\dot{\delta}_{\mu\vec{k}}|^2), \tag{44a}$$

$$D=\gamma\sum_{\vec{k}}\sum_{\mu}|\dot{\phi}_{\mu\vec{k}}|^2, \tag{44b}$$

$$R=\frac{1}{2}\sum_{\vec{k}}\sum_{\mu}(g_{\mu\vec{k}}^*\dot{\phi}_{\mu\vec{k}}+g_{\mu\vec{k}}\dot{\phi}_{\mu\vec{k}}^*). \tag{44c}$$

Since the $\vec{r}$-space functions are real, $\psi_{\vec{k}}^*=\psi_{-\vec{k}}$ for each of the $\phi_{\mu\vec{k}}$, $Q_{\mu\vec{k}}$, $\delta_{\mu\vec{k}}$, and $g_{\mu\vec{k}}$; consequently wave vectors $\vec{q}$ are only coupled to $-\vec{q}$, and we may write Eqs. (43) and (44) as a sum over half of $\vec{k}$ space, treating each wave vector independently.

One may write down the equations of motion (14) for arbitrary direction of the acoustic wave; this leads to a set of nine coupled differential equations which may be converted to nine coupled linear equations by Fourier transforming all variables in time. However, both in the calculation of the frequency of the acoustic wave and the dynamic structure factor, this is messy, and therefore we shall restrict ourselves to two particular directions of the wave vector—along the [100] and [110] directions—for which extensive experimental data exist.

A. Wave along [100] direction

In this case $k_x=k$, $k_y=k_z=0$. Then, keeping only the $\vec{k}$ and $-\vec{k}$ terms as explained above, we have

$$F_k=[a+(c_1+c_2)k^2]|\phi_{xk}|^2+(a+c_2k^2)(|\phi_{yk}|^2+|\phi_{zk}|^2)$$
$$+K_{11}k^2|\delta_{xk}|^2+K_{44}k^2(|\delta_{yk}|^2+|\delta_{zk}|^2)$$
$$+[ihk_x\delta_{xk}^*(Q_{yk}-Q_{zk})+\text{c.c.}]+(K_0+G)\sum_{\mu}Q_{\mu k}^*Q_{\mu k}$$
$$+f\sum_{\mu}(\phi_{\mu k}^*Q_{\mu k}+Q_{\mu k}^*\phi_{\mu k})+G\sum_{\mu\neq\nu}Q_{\mu k}^*Q_{\nu k}. \tag{45a}$$

Transforming to the variables

$$\phi_\pm=(\phi_{yk}\pm\phi_{zk})/\sqrt{2} \tag{46}$$

and $Q_\pm$ defined similarly, we get

$$F_k=[a+(c_1+c_2)k^2]|\phi_{xk}|^2+(a+c_2k^2)(|\phi_+|^2+|\phi_-|^2)$$
$$+K_{11}k^2|\delta_{xk}|^2+K_{44}k^2(|\delta_{yk}|^2+|\delta_{zk}|^2)$$
$$+\sqrt{2}\,ihk(\delta_{xk}^*Q_--Q_-^*\delta_{xk})+(K_0+G)|Q_{xk}|^2$$
$$+(K_0+2G)|Q_+|^2+K_0|Q_-|^2+\sqrt{2}\,G(Q_{xk}^*Q_++Q_+^*Q_{xk})$$
$$+f(\phi_{xk}^*\phi_{xk}+\phi_+^*Q_++\phi_-^*Q_-+\text{c.c.}). \tag{45b}$$

Expressions for the other terms in the dynamical equations are

$$K_k=M(|\dot{Q}_{xk}|^2+|\dot{Q}_+|^2+|\dot{Q}_-|^2)+m\sum_{\mu}|\dot{\delta}_{\mu k}|^2, \tag{47a}$$

$$D_k=2\gamma(|\dot{\phi}_{xk}|^2+|\dot{\phi}_+|^2+|\dot{\phi}_-|^2), \tag{47b}$$

$$R_k=[g_{xk}^*\dot{\phi}_{xk}+(2)^{-1/2}(g_{yk}^*+g_{zk}^*)\dot{\phi}_+$$
$$+(2)^{-1/2}(g_{yk}^*-g_{zk}^*)\dot{\phi}_-]+\text{c.c.} \tag{47c}$$

The equations of motion are obtained easily; Fourier transforming all variables in time, i.e.,

$$\psi_k(t)=\frac{1}{2\pi}\int d\omega\,\psi_k(\omega)e^{i\omega t}, \tag{48}$$

we obtain the set of equations

$$\begin{bmatrix} a+c_2k^2+i\omega\gamma & f & 0 & 0 & 0 & 0 & 0 & 0 & 0 \\ f & K_0-M\omega^2 & -\sqrt{2}ihk & 0 & 0 & 0 & 0 & 0 & 0 \\ 0 & \sqrt{2}ihk & K_{11}k^2-m\omega^2 & 0 & 0 & 0 & 0 & 0 & 0 \\ 0 & 0 & 0 & a+(c_1+c_2)k^2+i\omega\gamma & 0 & f & 0 & 0 & 0 \\ 0 & 0 & 0 & 0 & a+c_2k^2+i\omega\gamma & 0 & f & 0 & 0 \\ 0 & 0 & 0 & f & 0 & K_0+G-M\omega^2 & \sqrt{2}G & 0 & 0 \\ 0 & 0 & 0 & 0 & f & \sqrt{2}G & K_0+2G-M\omega^2 & 0 & 0 \\ 0 & 0 & 0 & 0 & 0 & 0 & 0 & K_{44}k^2-m\omega^2 & 0 \\ 0 & 0 & 0 & 0 & 0 & 0 & 0 & 0 & K_{44}k^2-m\omega^2 \end{bmatrix} \begin{bmatrix} \phi_- \\ Q_- \\ \delta_x \\ \phi_x \\ \phi_+ \\ Q_x \\ Q_+ \\ \delta_y \\ \delta_z \end{bmatrix} = \begin{bmatrix} \frac{g_{yk}-g_{xk}}{\sqrt{2}} \\ 0 \\ 0 \\ g_{xk} \\ \frac{g_{yk}+g_{xk}}{\sqrt{2}} \\ 0 \\ 0 \\ 0 \\ 0 \end{bmatrix}. \quad (49)$$

δ_y and δ_z, the transverse [100] waves, are found to decouple completely, and therefore show no pretransition effects. (Thus the shear elastic modulus C_{44} is equal to the unmodified K_{44}, and temperature independent, as in the static theory.) The equation for the longitudinal [100] wave is easy to decouple; the result is

$$\{(a+c_2k^2+i\omega\gamma)[(K_{11}k^2-m\omega^2)(K_0-M\omega^2)-2h^2k^2] - f^2(K_{11}k^2-m\omega^2)\}\delta_{xk}=ihkf(g_{xk}-g_{yk}). \quad (50)$$

The frequency of this mode is given simply by the zero of the left-hand side of the equation. For small values of k, we may assume that the zero of interest is much below the optic frequency $(K_0/M)^{1/2}$ and so the term $M\omega^2$ may be omitted in comparison with K_0. If one further neglects the width of the mode (which is not a bad approximation for the longitudinal [100] mode, which does not go totally soft), one obtains, for the acoustic frequency, the expression

$$\omega_k^2=\frac{C_{11}}{m}k^2\left(1-\frac{2h^2f^2/K_0^2C_{11}}{a_r+c_2k^2+3h^2f^2/(C_{11}-C_{12})K_0^2}\right), \quad (51)$$

where we have expressed the result in terms of the physical constants C_{ij} and a_r, related to the unrenormalized ones K_{ij} and a by Eqs. (24) and (26). The frequency far away from the transition is simply $\omega_{k\infty}=(C_{11}/M)^{1/2}k$, as it should be. At the transition temperature, in the long-wavelength limit, Eq. (51) reduces to

$$\omega_k^2=\frac{C_{11}}{m}k^2\left(1-\frac{2(C_{11}-C_{12})}{3C_{11}}\right)=\omega_{k\infty}^2\left(1-\frac{2(C_{11}-C_{12})}{3C_{11}}\right). \quad (52)$$

Thus the frequency at long wavelengths is reduced by the presence of the additional factor, which turns out to be 0.6–0.65 for both V_3Si and Nb_3Sn.

The temperature variation of the [100] longitudinal sound velocity $(k\to 0)$ follows directly from Eq. (51):

$$v(T)=v_\infty\left(1-\frac{2(C_{11}-C_{12})/3C_{11}}{1+\beta\theta}\right)^{1/2}, \quad (53)$$

where β is the coupling constant defined in Eq. (28), and θ is the reduced temperature, Eq. (27).

B. Wave along [110] direction

Here $k_x = k_y = k/\sqrt{2}$, $k_z = 0$. We write the free energy and other quantities in terms of the variables

$$\phi_1 = \frac{\phi_{kx} + \phi_{ky} + \phi_{kz}}{\sqrt{3}},$$

$$\phi_2 = \frac{\phi_{kx} - \phi_{ky}}{\sqrt{2}}, \tag{54}$$

$$\phi_3 = \frac{\phi_{kx} + \phi_{ky} - 2\phi_{kz}}{\sqrt{6}};$$

Q_1, Q_2, and Q_3 defined similarly in terms of Q_{xk}, Q_{yk}, and Q_{zk};

$$\delta_\pm = (\delta_{xk} \pm \delta_{yk})/\sqrt{2} \tag{55}$$

and δ_{zk}. Then

$$\begin{aligned} F_k = {} & (a + c_2k^2 + \tfrac{1}{3}c_1k^2)\,|\phi_1|^2 + (a + c_2k^2 + \tfrac{1}{2}c_1k^2)\,|\phi_2|^2 \\ & + (a + c_2k^2 + \tfrac{1}{6}c_1k^2)\,|\phi_3|^2 \\ & + (1/3\sqrt{2})c_1k^2(\phi_1^*\phi_3 + \phi_3^*\phi_1) \\ & + f(\phi_1^*Q_1 + \phi_2^*Q_2 + \phi_3^*Q_3 + \text{c.c.}) \\ & + (K_0 + 3G)\,|Q_1|^2 + K_0(|Q_2|^2 + |Q_3|^2) \\ & + \tfrac{1}{2}(K_{11} + 2K_{44} + K_{12})k^2\,|\delta_+|^2 + \tfrac{1}{2}(K_{11} - K_{12})k^2\,|\delta_-|^2 \\ & + K_{44}k^2\,|\delta_{zk}|^2 + (\tfrac{3}{2})^{1/2}ihk(\delta_-^*Q_3 - \delta_-Q_3^*) \\ & - (ihk/\sqrt{2})(\delta_+^*Q_2 - \delta_+Q_2^*), \end{aligned} \tag{56a}$$

$$K_k = M(|\dot{Q}_1|^2 + |\dot{Q}_2|^2 + |\dot{Q}_3|^2) + m(|\dot{\delta}_+|^2 + |\dot{\delta}_-|^2 + |\dot{\delta}_{zk}|^2), \tag{56b}$$

$$D_k = 2\gamma(|\dot{\phi}_1|^2 + |\dot{\phi}_2|^2 + |\dot{\phi}_3|^2), \tag{56c}$$

$$R_k = \frac{g_{xk}^* + g_{yk}^* + g_{zk}^*}{\sqrt{3}}\,\dot{\phi}_1 + \frac{g_{xk}^* - g_{yk}^*}{\sqrt{2}}\,\dot{\phi}_2 + \frac{g_{xk}^* + g_{yk}^* - 2g_{zk}^*}{\sqrt{6}}\,\dot{\phi}_3 + \text{c.c.} \tag{56d}$$

The equation of motion are

$$\begin{bmatrix} a + c_2k^2 + \frac{1}{2}c_1k^2 + i\omega\gamma & f & 0 & 0 & 0 & 0 & 0 & 0 & 0 \\ f & K_0 - M\omega^2 & ihk/\sqrt{2} & 0 & 0 & 0 & 0 & 0 & 0 \\ 0 & -ihk/\sqrt{2} & \frac{1}{2}(K_{11} + 2K_{44} + K_{12})k^2 - m\omega^2 & 0 & 0 & 0 & 0 & 0 & 0 \\ 0 & 0 & 0 & a + c_2k^2 + \frac{1}{3}c_1k^2 + i\omega\gamma & f & (3\sqrt{2})^{-1}c_1k^2 & 0 & 0 & 0 \\ 0 & 0 & 0 & f & K_0 + 3G - M\omega^2 & 0 & 0 & 0 & 0 \\ 0 & 0 & 0 & (3\sqrt{2})^{-1}c_1k^2 & 0 & a + c_2k^2 + \frac{1}{6}c_1k^2 + i\omega\gamma & f & -(\tfrac{3}{2})^{1/2}ihk & 0 \\ 0 & 0 & 0 & 0 & 0 & f & K_0 - M\omega^2 & (\tfrac{3}{2})^{1/2}ihk & 0 \\ 0 & 0 & 0 & 0 & 0 & 0 & -(\tfrac{3}{2})^{1/2}ihk & \frac{1}{2}(K_{11} - K_{12})k^2 - m\omega^2 & 0 \\ 0 & 0 & 0 & 0 & 0 & 0 & 0 & 0 & K_{44}k^2 - m\omega^2 \end{bmatrix} \begin{bmatrix} \phi_2 \\ Q_2 \\ \delta_+ \\ \phi_1 \\ Q_1 \\ \phi_3 \\ Q_3 \\ \delta_- \\ \delta_z \end{bmatrix} = \begin{bmatrix} \frac{g_{xk} - g_{yk}}{\sqrt{2}} \\ 0 \\ 0 \\ \frac{g_{xk} + g_{yk} + g_{zk}}{\sqrt{3}} \\ 0 \\ \frac{g_{xk} + g_{yk} - 2g_{zk}}{\sqrt{6}} \\ 0 \\ 0 \\ 0 \end{bmatrix} \tag{57}$$

The transverse [110] mode polarized along [001] decouples and thus shows no softening at the transition, in agreement with experiment. The longitudinal [110] phonon shows some softening, and by just comparing the matrix for this case with the longitudinal phonon, we can write down its frequency (under the same assumptions)

$$\omega_k^2 = \frac{C_{11}+2C_{44}+C_{12}}{2m}k^2 \times\left[1-\frac{h^2f^2}{K_0^2(C_{11}+2C_{44}+C_{12})}\Big/\left(a_r+(\tfrac{1}{2}c_1+c_2)k^2+\frac{3h^2f^2/K_0^2}{C_{11}-C_{12}}\right)\right], \tag{58}$$

which predicts finite velocities at $T=T_m^*$, and a softening even less than the [100] longitudinal case, as found experimentally.

To deal with the transverse [110] phonon polarized along [1$\bar{1}$0] (δ_-), we consider the case where the wavelength is long enough to permit us to neglect the off-diagonal $\phi_1\phi_3$ terms, which contribute $O(k^4)$ terms. Then ϕ_1 and Q_1 drop out of consideration and we obtain the equation

$$\begin{aligned}&((a+c_2k^2+\tfrac{1}{6}c_1k^2+i\omega\gamma)\{(K_0-M\omega^2)\\ &\qquad\times[\tfrac{1}{2}(K_{11}-K_{12})k^2-m\omega^2]-\tfrac{3}{2}h^2k^2\}\\ &-f^2[\tfrac{1}{2}(K_{11}-K_{12})k^2-m\omega^2])\delta_-\\ &\qquad=\tfrac{1}{2}ihkf(g_{xk}+g_{yk}-2g_{zk}).\end{aligned} \tag{59}$$

The sound velocity ($k\to 0$) is easily obtained by dropping all the k- and ω-dependent terms except $[\frac{1}{2}(K_{11}-K_{12})k^2-m\omega^2]$. The result is

$$\omega_k^2=[(C_{11}-C_{12})/2m]k^2[1-(1+\beta\theta)^{-1}], \tag{60a}$$

or

$$v(T)=v_\infty[1-(1+\beta\theta)^{-1}]^{1/2}, \tag{60b}$$

where

$$v_\infty=[(C_{11}-C_{12})/2m]^{1/2} \tag{61}$$

is the sound velocity far from the transition. Note that $v(T)$ and v_∞ in Eq. (53) refer to the [100] longitudinal wave and should not be confused with the ones in Eq. (60b).

It is tempting to write down an expression for the frequency at somewhat larger wave vectors in the manner we arrived at Eq. (51); however, since this mode goes totally soft at T_m^* in the quadratic approximation, we cannot neglect the width term $i\omega\gamma$, and in order to arrive at a correct expression for the frequency, we must compute the dynamic structure factor, which is just the Fourier transform of the correlation function $\langle\delta_-^*(t)\,\delta_-(t')\rangle$. To do that we calculate the correlation function for a particular random force g_k^n using Eq. (59), and then average over the ensemble of functions g_k^n, according to Eq. (13). The result is

$$S_\delta(k,\omega)=6h^2k^2f^2k_BT/[((a+\tfrac{1}{6}c_1k^2+c_2k^2)\{[(K_{11}-K_{12})k^2-m\omega^2](K_0-M\omega^2)-3h^2k^2\}-f^2[(K_{11}-K_{12})k^2-m\omega^2])^2 +\omega^2\gamma^2\{[(K_{11}-K_{12})k^2-m\omega^2](K_0-M\omega^2)-3h^2k^2\}^2]\ . \tag{62}$$

We are interested in small k, when the acoustic frequencies are much smaller than the optic ones. For the region of interest ($\omega\sim\omega_k$, the acoustic frequency), we may neglect $M\omega^2$ in comparison with K_0, and then the expression (62) may be put in the form

$$S_\delta(k,\omega)\simeq\frac{2\Omega k_BT/(C_{11}-C_{12})k^2}{[(\tau_k)^{-1}(1-x^2)-\Omega x^2]^2+\omega_{k\infty}^2x^2(1-x^2)^2}, \tag{63}$$

where

$$\tau_k\equiv\tau_k(T)=\gamma/[a_r+(\tfrac{1}{6}c_1+c_2)k^2] \tag{64a}$$

is a relaxation-time characteristic of the dissipation process, which diverges like $(T-T_m^*)^{-1}$ at the actual transition temperature T_m^* (in the quadratic approximation) for vanishing k;

$$\Omega=3h^2f^2/K_0^2\gamma(C_{11}-C_{12}) \tag{64b}$$

is a frequency characteristic of the coupling terms;

$$\omega_{k\infty}=[(C_{11}-C_{12})/2m]^{1/2}k \tag{64c}$$

is the acoustic frequency far from the transition, and $x=\omega/\omega_{k\infty}$ is the reduced frequency.

Equation (63) results directly from the equations of motion, and is valid for $x\ll(K_0/M\omega_k^2)^{1/2}$. For small k, the term on the right-hand side is much larger than unity, while the region of interest is $x\sim 1$, so this is not much of a restriction. The expression (63) is formally identical to the one obtained by the authors for the transition-metal dichalcogenides; however, because the anomaly here is at $k=0$, the results are qualitatively different. In the long-wavelength limit ($k\to 0$),

$S_\delta(k,\omega)$ exhibits a peak at the frequency given by Eq. (60a), which vanishes at $T=T_m^*$. The attenuation of the wave in this limit is easy to calculate, and the resultant mean-free path turns out to be

$$\Lambda_k=[(1+\Omega\tau_0)^{1/2}/\omega_k^2\tau_0^2\Omega]v_\infty, \tag{65}$$

where v_∞ is defined in Eq. (61) and $\tau_0=\tau_{k=0}(T)$. The above expression is valid as long as the k-dependent term in τ_k is small compared to the constant part, which translates to the condition $\omega_k^2 \ll 10^{25}\theta^2$, where θ is the reduced temperature (27), using values obtained by comparison with experiment (Sec. VII). This is satisfied by ultrasonic frequencies up to about $\frac{1}{10}$ of a degree from the transition.

For higher wave vectors, the behavior of $S_\delta(k,\omega)$ is dependent on the various parameters. If we assume that k^4 terms are not important, then basically two cases arise

$$\text{(a)}\quad \omega_{k\infty}^2 < 2\Omega/\tau_k(T_m^*) \tag{66a}$$

$$\text{(b)}\quad \omega_{k\infty}^2 > 2\Omega/\tau_k(T_m^*) \tag{66b}$$

At any given temperature $T>T_m^*$, in case (a), $S_\delta(k,\omega)$ has two peaks at the frequencies given by Eq. (60a) in the long-wavelength limit. As k is increased, the peak shifts to higher values of $x=\omega_k/\omega_{k\infty}$, according to the relation

$$x^2=\frac{1}{3}\left(\left\{\left[\left(\frac{1}{\omega_{k\infty}\tau_k}+\frac{\Omega}{\omega_{k\infty}}\right)^2-2\right]^2+3\left[\frac{2}{\omega_{k\infty}\tau_k}\left(\frac{1}{\omega_{k\infty}\tau_k}+\Omega\right)-1\right]\right\}^{1/2}-\left(\frac{1}{\omega_{k\infty}\tau_k}+\frac{\Omega}{\omega_{k\infty}}\right)^2+2\right), \tag{67}$$

which may be put into a form analogous to Eq. (51) by expanding it in powers of k^2 and retaining only up to $O(k^2)$ terms

$$\omega_k^2 \simeq \omega_{k\infty}^2[1-(1+\beta\theta+\eta k^2)^{-1}], \tag{68}$$

where

$$\eta=\frac{(\frac{1}{6}c_1+c_2)-\gamma v_\infty^2/2\Omega}{\Omega\gamma}+O(T-T_m^*). \tag{69}$$

v_∞ and Ω are defined in Eqs. (61) and (64b). Comparing Eqs. (68) and (51) we see that the main effect of retaining the width of the mode is a modification of the coefficient η. While Eq. (68) is approximate, its result is exact both in the small-k and high-θ limit, and can therefore be used to fit experimental curves instead of Eq. (67) in the entire range.

In case (b) the situation is more complex. Near the transition, as k increases from zero, the peak moves to smaller x (negative dispersion) and $S_\delta(k,\omega)$ has only a central ($\omega=0$) peak for intermediate k. As k is increased further, additional peaks develop for $x^2 \lesssim 1$, which increase in size with k, and take away all the spectral weight from the central peak which eventually disappears. At higher temperatures, the height of the central peak goes down roughly as $(T-T_m^*)^{-2}$ and the integrated intensity as $(T-T_m^*)^{-1}$. For still higher temperatures, depending on the extent of the inequality Eqs. (66), the behavior changes to Eq. (66a) where the central peak is absent for all k. The qualitative behavior of $S_\delta(k,\omega)$ in the two cases are displayed in Fig. 5 and schematic dispersion curves in Fig. 6.

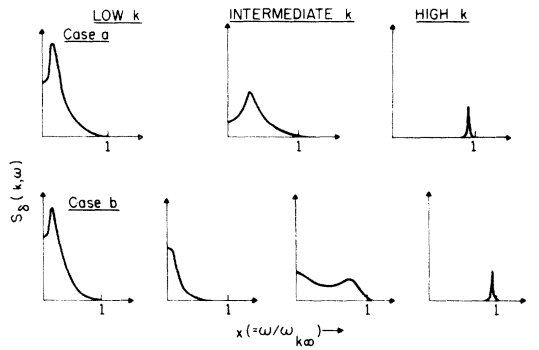

FIG. 5. Qualitative behavior of the acoustic structure function $S_\delta(k,\omega)$ for the $[1\bar{1}0]$ transverse mode, polarized along $1\bar{1}0$ for a given temperature $T \gtrsim T_m^*$ for different values of the wave vector, for the two cases (a) and (b) of Eqs. (66).

While it is tempting to associate the A-15 compounds with Eq. (66b) in light of the observed central peak in Nb_3Sn by neutron scattering, the net experimental evidence seems to be in favor of Eq. (66a). In fact, in Eq. (66b), the acoustic phonons in ultrasonic measurements and neutron measurements near the transition are different, and phonons in the latter should show very little softening, contrary to experimental evidence; also, the dispersion for ultrasonic phonons is predicted to be negative. The divergence associated with the central peak is also not in accord with experimental results.

The $\langle Q_3 Q_3 \rangle$ correlation function may be calculated in an analogous manner and leads to the ex-

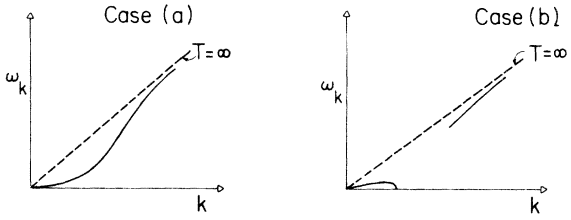

FIG. 6. Dispersion curves for the transverse [110] phonon (polarized $[1\bar{1}0]$) for Eqs. (66).

pression

$$S_Q(k,\omega)=\{[\tfrac{1}{2}(K_{11}-K_{12})k^2-m\omega^2]^2/\tfrac{3}{2}h^2k^2\}S_\delta(k,\omega). \tag{70}$$

Thus $S_Q(k,\omega)$ exhibits basically the same behavior as $S_\delta(k,\omega)$, except that the acoustic peak is suppressed at long wavelengths by a factor k^2, while the optic peak is enhanced by the same factor. In the $k=0$ limit, Eq. (70) leads to

$$S_Q(0,\omega)=\frac{4\Omega' k_B T/\gamma K_0}{[(\tau_0)^{-1}(1-x^2)+\Omega-\Omega' x^2]^2+\omega_0^2 x^2(1-x^2)^2}, \tag{71}$$

where $\tau_0(T)$ and Ω have been defined in Eqs. (64a) and (64b);

$$\Omega'=\Omega+f^2/K_0\gamma \tag{72a}$$

is another characteristic frequency of the system,

$$\omega_0=(K_0/M)^{1/2} \tag{72b}$$

is the optic frequency far from the transition, and $x=\omega/\omega_0$ is the reduced frequency [different from Eq. (63)].

Far from the transition, $S_Q(0,\omega)$ exhibits peaks at $x^2=1$, as expected. As the temperature is lowered, the peaks shift to lower values of $|x|$. In the large dissipation case, $(2\Omega\Omega'<\omega_0^2)$, a central peak appears, and rises in height to a finite (nondivergent) value at T_m^*. For small Ω', the optic peak remains at a finite value of x. However, if Ω' gets close in value to $\sqrt{2}\,\omega_0$, so that $(\Omega'^2-2\omega_0^2)^2<3(\omega_0^2-2\Omega\Omega')$, then the optic mode goes totally soft, and merges into the central peak at a temperature above T_m^*; the same behavior ensues for all higher Ω', so long as the large dissipation condition is satisfied. In the weak dissipation case $(2\Omega\Omega'>\omega_0^2)$, the optic mode has a finite frequency all the way up to T_m^*, and no central peak is present for any $T\geq T_m^*$.

VI. IMPURITY EFFECTS

Impurity effects on charge-density-wave transitions are fairly well understood from the work on transition-metal dichalcogenides.[15a] The impurity potential creates a charge-density-wave cloud around the impurity even in the normal state. This cloud can be observed as a diffuse peak in x-ray or neutron scattering and is one source of the "central peak." We compute the impurity contribution to the correlation function $\langle\delta(\vec{r})\delta(\vec{r}')\rangle$ by obtaining the result for a given impurity distribution with potential $u(\vec{r})$ and then averaging over an ensemble. We write the free energy in $\vec{k}$ space as in Sec. V; this time including the coupling to the impurity potential. Modes for different wave vectors decouple as before, and we consider the case for $\vec{k}$ along the [110] direction, where the central peak has been observed experimentally. The only relevant mode near the phase transition is the linear combination of ϕ_3, Q_3, and δ_- [e_3 of Eq. (21)], which goes soft at T_m^*. Omitting the off-diagonal $\phi_1\phi_3$ terms as before, the relevant portion of the free energy (up to quadratic terms) becomes of the form [notation of Eq. (57)]

$$F_k=[a+(c_2+\tfrac{1}{6}c_1)k^2]|\phi_3|^2+K_0|Q_3|^2+f(\phi_3^*Q_3+Q_3^*\phi_3)+\left(\frac{3}{2}\right)^{1/2}ihk(\delta_+^*Q_3-\delta_-Q_3^*)+\tfrac{1}{2}(K_{11}-K_{12})k^2|\delta_-|^2+(u_{k3}\phi_3^*+u_{k3}^*\phi_3), \tag{73}$$

where

$$u_{k3}=\int d^3r\, e^{i\vec{k}\cdot\vec{r}}\,\frac{u_x(\vec{r})+u_y(\vec{r})-2u_z(\vec{r})}{\sqrt{6}} \tag{74}$$

with $\vec{k}=(kk0)/\sqrt{2}$ in this case.

Minimizing F_k with respect to ϕ_3^*, Q_3^*, and δ_+^* and solving for δ_- we get

$$\delta_-=\frac{-\sqrt{6}\,ihfu_{k3}/k}{K_0(C_{11}-C_{12})[a_r+(c_2+\tfrac{1}{6}c_1)k^2]}, \tag{75}$$

so that the structure factor is

$$S_\delta(k)=\langle\delta_+^*\delta_-\rangle=\frac{6h^2f^2\langle u_{k3}^*u_{k3}\rangle}{k^2K_0^2(C_{11}-C_{12})^2[a_r+(c_2+\tfrac{1}{6}c_1)k^2]^2}. \tag{76}$$

While the ensemble average of u_{k3} vanishes, $\langle u_{k3}^*u_{k3}\rangle$ does not, and so for small k, the structure factor has a central ($\omega=0$) peak due to impurity scattering whose intensity diverges as $(T-T_m^*)^{-2}$.

Equation (76) may be put in a form which facilitates comparison with experiment [$I\propto k^2S_\delta(k)$]:

$$\frac{1}{\sqrt{I}}=\text{const}\left((T-T_m^*)+\frac{c_1/6+c_2}{a'}\,k^2\right). \tag{77}$$

Regarding the attenuation of the transverse [110] phonon polarized [1$\bar{1}$0] due to impurities, one can extract the dependence on temperature from the following qualitative argument.

For a single impurity at the origin the perturbation to the Hamiltonian is of the form

$$\Delta\mathcal{H}=p_0^2\left(\frac{1}{2M'}-\frac{1}{2M}\right)+\sum_i\sum_{\alpha,\beta=x,y,z}\Delta K_i^{\alpha\beta}x_0^\alpha x_i^\beta. \tag{78}$$

The temperature dependence of the attenuation for both terms (for constant frequency) is the same, as will be apparent later in the argument, so we consider only the first term which is easier to deal with. In terms of phonon creation and annihilation operators, that term is of the form

$$\Delta\mathcal{H}_1 \sim \sum_{\sigma,\sigma'} \sum_{\vec{k},\vec{q}} (\omega_{\vec{k}\sigma}\omega_{\vec{q}\sigma'})^{1/2}(a_{\vec{k}\sigma} - a^{\dagger}_{\vec{k}\sigma})(a_{\vec{q}\sigma'} - a^{\dagger}_{\vec{q}\sigma'}), \tag{79}$$

where σ,σ' denote polarization.

From Fermi's golden rule, the rate of the transition (phonon of wave vector $\vec{k}$, $\sigma \rightarrow$ anything) is

$$\Gamma_{\vec{k}\sigma} \sim \sum_f |\langle f|\Delta\mathcal{H}_1|\vec{k}\sigma\rangle|^2 \delta(\omega_f - \omega_{\vec{k}\sigma}), \tag{80}$$

if we consider only elastic scattering. The only final states to be considered then are one-phonon states and we get

$$\Gamma_{\vec{k}\sigma} \sim \sum_{\sigma'} \int q^2 dq\, d(\cos\theta) d\phi\, \omega_{\vec{k}\sigma}\omega_{\vec{q}\sigma'}\delta(\omega_{\vec{k}\sigma} - \omega_{\vec{q}\sigma'}). \tag{81}$$

At this stage we use a model dispersion curve to emulate the A-15 compound case. One suitable choice is to take the transverse polarization with $\sigma = [1\bar{1}0]$ for $\hat{k} = [110]$ with a dispersion

$$\omega_{q\sigma} \sim q[\sin^2\theta + (T - T_m^*)]^{1/2}, \tag{82}$$

where θ is the angle with [110] direction as the polar axis of integration, and the remaining $\omega_{q\sigma'}$ $(\sigma' \neq \sigma)$ are taken to be temperature independent. Then the transformation of variables from q to $\omega_{q\sigma'}(\sigma' \neq \sigma)$ is temperature independent and thus for constant $\omega_{k\sigma}$, the contribution to $\Gamma_{\vec{k}\sigma}$ is also temperature independent and uninteresting. For $\sigma' = \sigma$, transforming to $\omega_{q\sigma}$ as an integration variable we get

$$\Gamma_{\vec{k}\sigma} \sim \omega_{\vec{k}\sigma}^4 \int_{-1}^{+1} \frac{d(\cos\theta)}{[\sin^2\theta + \alpha(T - T_m^*)]^{3/2}},$$
$$\Gamma_{\vec{k}\sigma} \sim \omega_{\vec{k}\sigma}^4 / (T - T_m^*)^{1/2} \tag{83}$$

which leads to an attenuation equal to

$$\Gamma_{\vec{k}\sigma}/v_{\vec{k}\sigma} \sim \omega_{\vec{k}\sigma}^4/(T - T_m^*). \tag{84}$$

For the other term, by proceeding similarly we can see that the $(T - T_m^*)^{-1}$ dependence comes out, though the ω dependence is different. Also, the essential point of the dispersion curve (82) is the $(T - T_m^*)^{1/2}$ dependence of $\omega_{\vec{q}\sigma}$ for a [110] transverse wave polarized $[1\bar{1}0]$ and the θ^2 dependence around the [110] axis for the elastic constant.

In the CDW state in transition-metal dichalcogenides,[15a] the impurities pin the CDW and strongly depress the lock-in transition. Impurities on the transition-metal sites have a strong effect on the CDW, whereas the nontransition atom site impurities have only a weak effect. We expect this experience to carry over to the A-15 compounds—the martensitic transition is expected to be strongly suppressed by impurities on the transition-metal (A) sites, but only weakly affected by impurities on the B sites. This is in fact the case, and the martensitic transition has been observed in B-site alloys like $Nb_3Sn_{1-x}Sb_x$ and $Nb_3Ge_{1-x}Al_x$.

VII. COMPARISON WITH EXPERIMENT

In this section, we compare the predictions of our model with experimental results; as a consequence of the fitting, we are able to obtain many of the parameters of the Landau theory.

A. Elastic softening

According to our model, the only temperature-dependent elastic constant is $[C_{11}(T) - C_{12}(T)]$. Experimental results on V_3Si and Nb_3Sn indicate that this bulk modulus $[C_{11}(T) + 2C_{12}(T)]$ is only weakly temperature dependent, while $C_{44}(T)$ does show some softening (approximately 6% for V_3Si and 30% for Nb_3Sn), which can be explained[11] on the basis of interchain electronic coupling which we have omitted. Thus the results are qualitatively in agreement with experiment. Quantitative fits have been made to the transverse 110 sound velocity (polarization along $1\bar{1}0$), using Eq. (60b), and the results for both V_3Si and Nb_3Sn are shown in Fig. 7 (experimental data from Refs. 2 and 18).

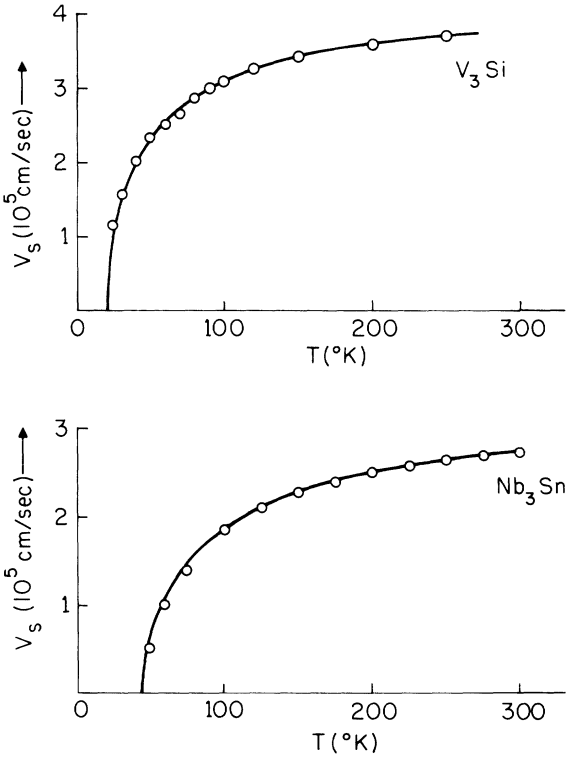

FIG. 7. Fits to the transverse [110] sound velocity (polarization $[1\bar{1}0]$) in V_3Si and Nb_3Sn as functions of temperature [Eq. (60b)] along with the experimental points computed from the data of Refs. 2 and 18.

The agreement is quite remarkable right up to room temperatures and shows that the experimental data are *not* conclusive evidence for a logarithmic dependence of elastic constants on temperatures as claimed by Gorkov. The effect of cubic terms which have been neglected is only within a few degrees of the transition, and explains why total softening is not observed in practice. From the fit, we obtain the constants

$$V_3Si \begin{cases} C_{11}-C_{12}=2.1\times10^{12}\ \text{dyn/cm}^2, \\ \beta=(C_{11}-C_{12})K_0^2a'T_m^*/3\hbar^2f^2=0.31, \end{cases}$$

$$Nb_3Sn \begin{cases} C_{11}-C_{12}=2.03\times10^{12}\ \text{dyn/cm}^2 \\ \beta=0.36. \end{cases}$$

It is interesting to note that β is approximately the same for both compounds, which says that the "healing" temperatures and transition temperatures are proportional.

Using the above-determined constants and the (constant) value of the bulk modulus from Testardi,[5] we fit the [100] longitudinal phonon velocities for V_3Si and Nb_3Sn in Fig. 8. The agreement is again very good, considering the fact that no additional parameters have been adjusted. From Eq. (58) we can compute the softening of the longitudinal [110] phonon to be about 10% for both V_3Si and Nb_3Sn; the experimental figure is close for V_3Si, but somewhat more than 15% for Nb_3Sn, which is due to the softening of C_{44}, not predicted by our model.

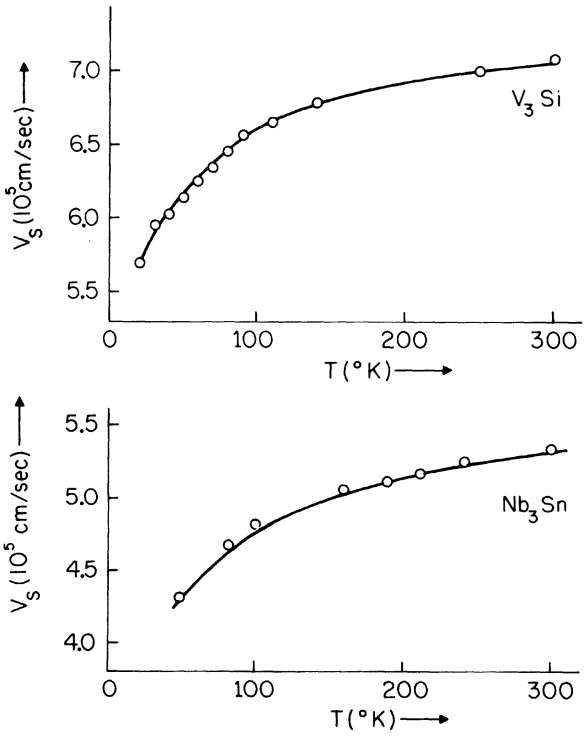

FIG. 8. [100] longitudinal sound velocity in V_3Si and Nb_3Sn as functions of temperature [Eq. (53)]. Points are computed from the data of Refs. 2 and 18.

B. Phonon dispersion

We next consider the dispersion curves for the transverse [110] phonon polarized along [1$\bar{1}$0] at different temperatures, as determined by neutron scattering.[3] The approximate formula, valid for small wave vectors, is Eq. (68). With β determined, we fit the curves with a single adjustable parameter η, and the results are shown in Figs. 9. We see that the phonon-dispersion curves near the transition bend upwards at small k, and asymptotically approach the high-temperature curves

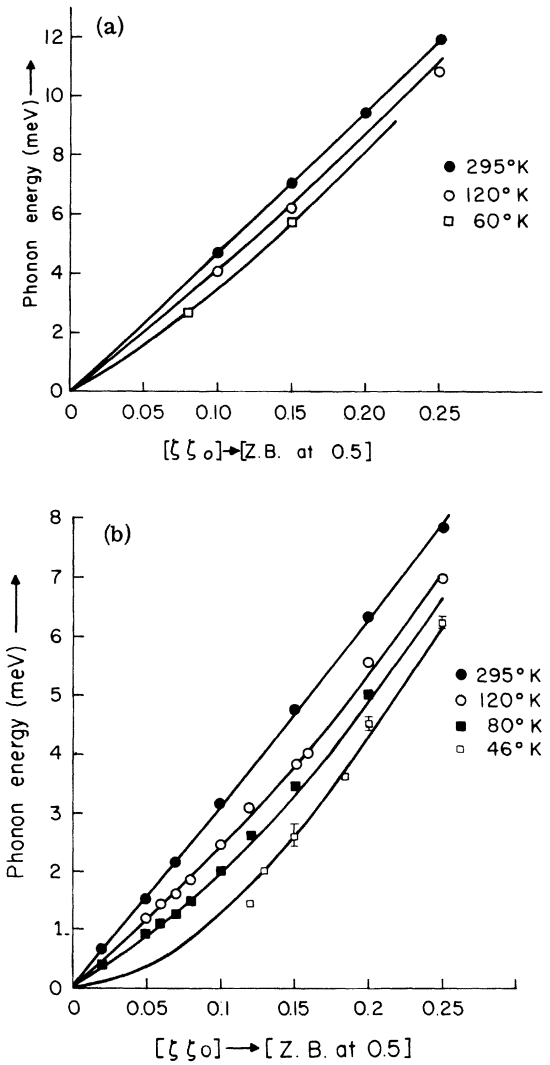

FIG. 9. Fits to the transverse [110] phonon (polarization [1$\bar{1}$0]) dispersion curves for (a) V_3Si and (b) Nb_3Sn, using Eq. (68) with a single adjustable parameter, η.

at high k. The values of η obtained from the fit are

$$\eta = \frac{(\frac{1}{6}c_1 + c_1) - \gamma v_\infty^2/2\Omega}{\Omega\gamma} \simeq \begin{cases} 12(a_0^2/8\pi^2)\ \mathrm{Nb_3Sn}, \\ 25(a_0^2/8\pi^2)\ \mathrm{V_3Si}, \end{cases}$$

where a_0 is the lattice spacing (in the cubic state). The result for V_3Si is approximate, since no data were available for temperatures near the transition. The correlation length ξ is given by $\xi = (\eta/\beta\theta)^{1/2}$, which, according to the Peierls model should be,

$$\xi \sim \frac{\hbar}{\Delta(T)}\left(\frac{dE_k}{dk}\right)_{E_F} \sim \frac{E_F a_0}{\Delta(T)}.$$

This implies $\eta \propto \beta a_0^2 (E_F/\Delta(0))^2$ or $\eta a_0^2 \sim T_m^{-2}$, if the band structures of V_3Si and Nb_3Sn were identical. Actually, $\eta a_0^2 \sim T_m^{-1}$ seems to be more in agreement with the fits, showing that there are some differences in the band structrues of the two compounds beyond just the effects of lattice size.

C. Ultrasonic attenuation

Equation (65) predicts an ω^2 and a $(T - T_m^*)^{-3/2}$ dependence of the attenuation of [110] shear ultrasonic waves (with $[1\bar{1}0]$ polarization) near T_m, which is in qualitative agreement with the experimental results in V_3Si.[2] However, as shown in Sec. VI, other means of attenuation such as impurity scattering are also enhanced near the transition temperature (simply because of the slowing down of the velocity), and thus a quantitative fit to experimental data does not yield any meaningful results. If we try to account for all the attenuation in terms of the dissipation term D, we obtain estimates of Ω [Eq. (64b)] and Ω' which imply a "central" peak in the optic structure function which would show up as pretransition forbidden (300) Bragg reflection above T_m, in disagreement with neutron scattering results. In fact, we may obtain an order of magnitude estimate for γ from resistivity data (Sec. VII J), and with that estimate, the magnitude of ultrasonic attenuation is much too low to explain the experiment, indicating that the electron charge-density relaxation processes are *not* the explanation of the high ultrasonic attenuation observed near the transition in V_3Si.

D. Static theory constants for Nb_3Sn

For Nb_3Sn, experimental data on the tetragonal deformation[19] indicate a first-order transition. The data yield a spontaneous deformation $\epsilon_3(T_m) \simeq 1.5\times10^{-3}$ and $(T_m - T_m^*) \simeq 4\ ^\circ\mathrm{K}$ [Eqs. (33) and (35)]. Comparison of theory with the temperature dependence of the central peak intensity for the [110] phonon with $[1\bar{1}0]$ transverse polarization[3a] (Sec. VII H) gives an estimate $(T_m - T_m^*) \simeq 2$–$3\ ^\circ\mathrm{K}$. Thus, precise magnitude of the cubic term is difficult to estimate; presumably it is somewhat sample dependent too. However, its effect at low temperatures is governed by the ratio $(T_m - T_m^*)T_m$ which is small. So we use the quadratic theory to determine the constants from the tetragonal and sublattice distortions at low temperatures. We shall, in this section, work with the energy gaps v_μ instead of the charge-density wave amplitudes ϕ_μ, which are simply proportional to each other, as explained in Sec. II. The corresponding parameters will be A' instead of a' and F instead of f. Any quantity involving only the combination (a'/f^2) will, of course, be the same in both cases.

The only coordinates to have nonzero values below T_m are ϵ_3, Q_2, and v_2, which are proportional to one another in the ratio given by e_2 of Eq. (21). At 4 °K, $\epsilon_3 = 0.0051$, while $Q_2 = 0.023$ Å.[3a] The gaps v_x and v_y are approximately $4k_B T_m \simeq 16$ meV, which yields

$$\frac{\sqrt{3}h/(C_{11} - C_{12})}{1 + 3h^2/K_0(C_{11} - C_{12})} = 0.22\ \text{Å}^{-1},$$

$$\sqrt{3}hF/K_0(C_{11} - C_{12}) = 0.23\ \text{eV}^{-1}.$$

With the value of β and $(C_{11} - C_{12})$ from Sec. VII A, we can obtain all the relevant static theory parameters for Nb_3Sn in terms of a dimensionaless variable $R = \sqrt{3}h/[K_0(C_{11} - C_{12})]^{1/2}$. The results are tabulated in Table I. As will be seen in Sec. VII J, the parameter R may be determined from the variation of the optic-mode frequency with temperatures, though it is likely to be of order unity.

For V_3Si, early measurements[20] put a limit on sublattice distortions of $Q_\mu < 0.005$ Å which gives a Q/ϵ ratio close to that of Nb_3Sn. Thus, higher resolution work is necessary to obtain the static theory parameters for V3Si.

TABLE I. Static theory parameters for Nb_3Sn. Values are expressed in terms of a number multiplied by a function of the dimensionless variable $R \equiv [3h^2/K_0(C_{11} - C_{12})]^{1/2}$, where the function has a value unity for $R = 1$.

Quantity	Value
A'	4.4×10^{-4} eV^{-1} Å^{-3} °K^{-1}
K_0	$0.24[(1+R^2)/2R]^2$ eV Å^{-5}
F	$0.13[(1+R^2)/2R^2]$ Å^{-4}
$(C_{11} - C_{12})$	1.3 eV Å^{-3}
h	$0.32[(1+R^2)/2R]$ eV Å^{-4}

E. Nonlinear stress-strain relation in V_3Si

For V_3Si, measurements of the tetragonal distortion[1] indicate "a rapid but smooth" change in the tetragonality near the transition, which implies that the transition is either second order, or very weakly first order. Putting $\alpha_3 = 0$, one can determine the ratio α_2'/α_4 from the measurement of the deformation at temperatures just above the superconducting transition, and the resultant (nonlinear) stress-strain plot at 25 °K obtained from Eq. (41) is shown along with the experimental measurements of Patel and Batterman[17b] in Fig. 10. The discrepancy that exists between the calculated curve and experiment may be resolved by the addition of a small cubic term which would cause a modification of the transition temperature of as low as 0.2 °K, and this explains the observed independence of the transition temperature[17a] on unaxial stress to within that limit. The corresponding spontaneous deformation (at T_m) is somewhat less than $\frac{1}{3}$ of the low-temperature value for V_3Si. However, because of the proximity of the superconducting transition temperature, a quantitative fit to the data is not very meaningful.

F. Heat-capacity data

Since the tetragonal deformation in the crystals is small, anomalies in the heat capacity are tiny and results are necessarily of limited reliability. Consequently, only a rough agreement with experiment is called for. For V_3Si, assuming the cubic term to be absent (parameters of Fig. 10), we obtain a specific-heat jump at the transition [Eq. (40)] of 0.7 J/mole deg, which compares favorably with the experimental value of 0.5 J/mole deg.[21a] Including the tiny cubic term necessary to obtain agreement with the nonlinear stress-strain curve would not affect results to any noticeable degree.

For Nb_3Sn, using the estimates $\alpha_3/\alpha_4 \sim 2.9 \times 10^{-3}$ and $(T_m - T_m^*) \sim 4$ °K (Ref. 19), we obtain a heat-capacity jump of 3 J/mole deg and a latent heat of approximately 3 J/mole, compared to the experimental anomaly of a jump of about 3 J/mole deg.[21b] No sharp latent heat peak is obtained experimentally; only a weak cusp, which indicates smearing of the transition.

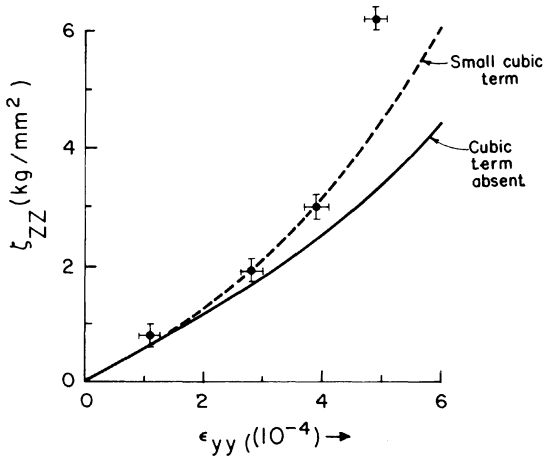

FIG. 10. Nonlinear relationship between uniaxial stress and transverse strain in V_3Si at 25°K calculated in the absence of a cubic term and with a small cubic term which would modify the transition temperature by 0.2° (dotted line), along with the experimental data (Ref. 17b).

G. Magnetic susceptibility drop below the transition

According to the Peierls transition model, the coefficient of the term quadratic in the gap in the free energy at absolute zero is equal to density of electron states of one spin at the Fermi surface which has been "pinched off" because of the gap. Since there are two chains participating in this case (v_x and v_y for a tetragonal deformation with c axis along z), the net change in susceptibility is expected to be (apart from any enhancement factors):

$$\Delta\chi = 2\mu_B{}^2 N(E_F) = 4\mu_B{}^2 \tfrac{1}{2} A' T_m ,$$

where μ_B is the Bohr magneton and $N(E_F)$ is the density of states for both spins at the Fermi surface for one chain.

With the estimate for A' from Table I, we arrive at $\Delta\chi \simeq 2.4 \times 10^{-7}$ emu/g for Nb_3Sn, which is in good agreement with the experimental value[18] of $\chi(T_m) - \chi(0) \simeq 2 \times 10^{-7}$ emu/g, considering the fact that the calculated value is based on the guess $v_\mu(0) = 4k_B T_m$ for the gap.

H. Intensity of central peak in neutron scattering

The results of Sec. VI predicted a $(T - T_m^*)^{-2}$ dependence for the intensity I of the central peak in the [110] transverse-acoustic structure function caused by impurities. A plot of $1/\sqrt{I}$ vs T for Nb_3Sn is shown in Fig. 11 and the straight-line fit predicted by Eq. (77) is in good agreement with the experimental data.[3a] With the estimate for the intercept coming from the fit to the [110] transverse phonon dispersion curve (Fig. 9), neglecting the renormalization of $(\frac{1}{6}c_1 + c_2)$ by the γ-dependent term (which is justified in lieu of the discussion in Sec. VII J), we obtain an estimate for the modification of the transition temperature due to the cubic term

$$T_m - T_m^* \simeq 2.5\ ^\circ\mathrm{K} ,$$

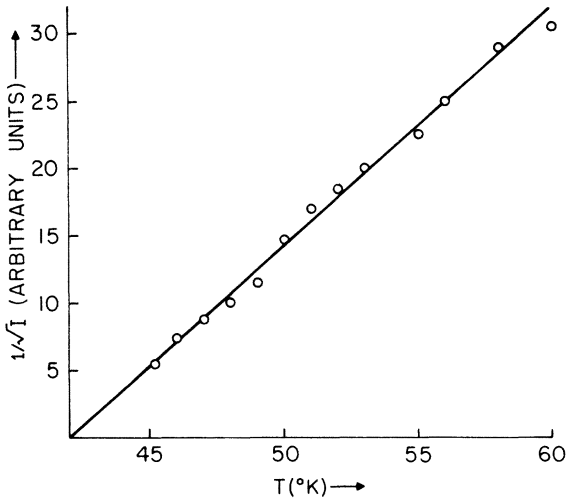

FIG. 11. Plot of the inverse half power of the central-peak intensity seen in neutron scattering (Ref. 3) for Nb_3Sn, vs the temperature. Straight line fit is predicted for central-peak intensity due to impurities.

which is in reasonable agreement with the estimate of 4 °K from fits to distortion curves. This reduction of 40% in $(T_m - T_m^*)$ entails about 20% reduction in the spontaneous deformation at T_m, which is within fitting accuracies.

I. Miscellaneous qualitative results: Effects of pressure, alloying

In this section, we give qualitative explanations for some experimental observations on the basis of our model. As shown at the end of Sec. IV, theory predicts a correlation between the variation of transition temperature with hydrostatic pressure and the sign of the tetragonality. This is in fact observed in V_3Si and Nb_3Sn. For the former with positive tetragonality, T_m is found to decrease with pressure[22a] while for Nb_3Sn with negative tetragonality, T_m is found to increase with pressure.[22b] We have already shown that the small variation of T_m with uniaxial stress is consistent with the nonlinear uniaxial-stress-transverse-strain data obtained near the transition temperature.

Our model also predicts the change in sign of tetragonality as a function of alloying, observed in the $Nb_3Sn_{1-x}Sb_x$ system[23] ($c/a = 0.9948$ in Nb_3Sn to 1.0048 in $Nb_3Sn_{0.85}Sb_{0.15}$). As shown in Fig. 3(b), the low-temperature strain jumps suddenly from positive to negative as the Fermi energy crosses the energy at the X point. This is because the sign of the cubic term determines the sign of the tetragonality, while it does not determine the magnitude [Eq. (37b)].

J. Dependence of the optic-mode frequency on temperature

Another result one can infer from the theory, for which no experimental data exists is a long-range temperature variation of the optic-mode frequency, though it does not go soft at T_m. In order to do so, one has to obtain an order of magnitude estimate for the coefficient γ of the dissipative term. A crude estimate may be made from the following argument.

If the electronic dissipation term D is responsible for the resistivity of the system, we may identify the dissipation per unit volume $\frac{1}{2}\gamma(\partial\phi/\partial t)^2$ as simply the Ohmic term $j^2/2\sigma$, where σ is the conductivity of the material. This in conjunction with the equation of continuity $\partial\rho/\partial t + \vec{\nabla}\cdot\vec{j} = 0$ leads to the estimate of γ as

$$\gamma = \rho_0^2/\sigma k^2 , \tag{85}$$

where k is the wave vector of the charge-density wave and ρ_0 is the electronic charge density in the normal state. Putting in estimates for various quantities yields $\gamma \sim 10^{-9}$ cgs for Nb_3Sn, and in turn for a reasonable value of the amplitude at $T = 0$ ($\phi(0) \sim 0.1$–0.2) leads to $\Omega \sim 10^{17}$–10^{18} Hz which is much higher than typical optic frequencies. For V_3Si, the estimate is smaller by about an order of magnitude, but still much higher than the optic-phonon frequency. This implies, for one, that the modification of the k^2 term by the dissipative process in Eq. (69) is very small, i.e., $\eta \simeq (\frac{1}{6}c_1 + c_2)/\Omega\gamma$. It also implies that the optic-phonon structure function [Eq. (71)] has no "central" peak, which is in agreement with the experimentally observed[3] *absence* of the "forbidden" (300) reflection right up to the transition in Nb_3Sn. Furthermore, the optic-phonon frequency is given essentially by the vanishing of the first term in the denominator of Eq. (71).

Using the parameters calculated in Sec VII D, and the estimate of twice the niobium atomic mass per cubic unit cell for M (the reduced mass $\frac{1}{2}m_{Nb}$ multiplied by four, since Q is $\frac{1}{2}$ the difference coordinate of neighboring niobium atoms on the linear chains), we arrive at the expression for the frequency of the optic phonon

$$\omega_{op} = (28\ \text{meV})[(1+R^2)/2R]\{1 - [(1+\beta\theta)R^2 + 1]^{-1}\}^{1/2} , \tag{86}$$

where

$$R = \sqrt{3}h/[K_0(C_{11} - C_{12})]^{1/2} . \tag{87}$$

$\beta = 0.36$, as per Sec. VII A, and $\theta = (T - T_m^*)/T_m^*$ is the reduced temperature. A plot of $\omega_{op}(T)$ vs T for three values of R is given in Fig. 12. Particularly noteworthy is the long-range variation of the frequency with temperature (healing temperature $\sim T_m/\beta$ for $R \gtrsim 1$ and $\sim T_m/\beta R^2$ for $R < 1$). While R

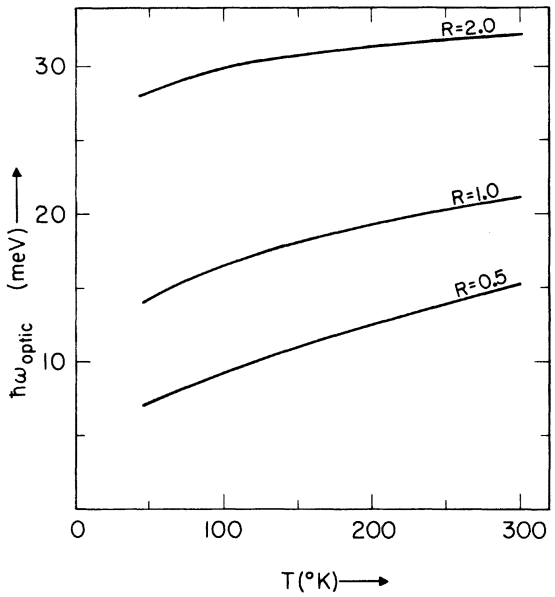

FIG. 12. Predicted temperature dependence of the Γ_{12} optic-phonon frequency in Nb_3Sn for different values of the dimensionless parameter $R \equiv \sqrt{3}h/[K_0(C_{11}-C_{12})]^{1/2}$.

is a measure of coupling of the optic phonon and the dilatation of the lattice ($R \to \infty$ corresponds to an unstable lattice), it should be kept in mind that the off-diagonal component is also present in β and the number 28 meV in front, and so that variation of $\omega_{op}(T)$ with R shown in Fig. 12 does not reflect the variation of $\omega_{op}(T)$ with off-diagonal terms directly.

VIII. RELATIONSHIP TO SUPERCONDUCTIVITY

The martensitic transformation affects the superconducting transition in two ways. Firstly, a significant fraction of the phonons soften as one moves toward the martensitic transition and stiffen after passing through it. The lattice softening increases the effective electron-phonon coupling constant and therefore increases the superconducting transition temperature. This has been appreciated for some time but the magnitude of the effect is unknown.

Secondly, the charge-density wave opens up a band gap on a portion of the Fermi surface that could otherwise have been used for pairing. This reduces the superconducting transition temperature in the tetragonal phase, as has been observed in V_3Si.[24] When the martensitic transition occurs just above the superconducting transition, as in V_3Si, there is an interesting interplay as the CDW gap and the BCS gap compete for the same piece of the Fermi surface. Considering both effects, one expects a maximum in the transition temperature when T_c and T_m are equal. This is observed in $Nb_3Sn_{1-x}Al_x$ alloys[25] where the highest T_c is found at the cubic-tetragonal boundary. In V_3Si, T_c and T_m approach each other at high pressure and one expects a maximum T_c at the intersection at about 25 kbar. If it occurs first, the superconducting transition should suppress the martensitic transition.

We expect that anything which enhances (suppresses) the martenistic transition temperature will suppress (enhance) the superconducting transition temperature. The pressure dependence of T_m and T_c in Nb_3Sn and V_3Si (Ref. 22) are consistent with these ideas. The model predicts that the signs of $(c/a-1)$, $dT_m dP$, and dT_c/dP are governed by the sign of $(E_F - E_x^0)$. For Nb_3Sn, E_F is below E_x^0 [since $(c/a-1)$ changes sign between Nb_3Sn and $Nb_3Sn_{0.85}Sb_{0.15}$], and $(c/a-1)<0$, $dT_m/dP>0$. This means that λ_1 is positive while λ_2 is negative. For V_3Si, the signs of $(c/a-1)$, dT_m/dP, and dT_c/dP are opposite to those for Nb_3Sn, and evidently E_F is above E_X^0 for V_3Si. This correlation should hold up for all the A-15 compounds.

Uniaxial stress also suppresses the superconducting transition by creating a CDW gap. Impurities, which are dressed with local CDW cloud, affect both transitions. The local band gap suppresses superconductivity in nontransforming samples in the same way that the uniform band gap does in transforming samples. Impurities broaden the martensitic transition and suppress it by creating a CDW gap of the wrong phase to pair the transition-metal atoms.

IX. CONCLUSIONS

To summarize, we have put forward a Landau theory for the martensitic transition in the A-15 compounds, using Gorkov's physical picture of a Peierls-like instability, and have made an extensive comparison of the results with experiment.

The theory explains the observed tetragonal distortion with a $\Gamma_{12}(+)$-type sublattice displacement, and the transition is expected to be weakly first order. The elastic behavior (except for the shear constant C_{44} whose (somewhat weaker) temperature can be accounted for in terms of interchain electronic terms) is well reproduced with a *nonlogarithmic* fit, as are the transverse [110] phonon dispersion curves. The central peaks in neutron scattering and ultrasonic attenuation are found not to be ascribable to electron dynamics, and at least the former is in agreement with impurity scattering.

Experimental results for V_3Si are consistent with a rather weakly discontinuous transition, while for Nb_3Sn, the transition is somewhat more

first order. The static theory constants for Nb_3Sn have been obtained from the measurements of the low-temperature strain and sublattice displacement.

The drop in susceptibility calculated on the basis of a Peierls transition model using the constants determined from the elastic behavior is in good agreement with the experimental result for Nb_3Sn. From a determination of the various parameters, the $\Gamma_{12}(+)$ optic-mode frequency is predicted to be temperature dependent right up to room temperatures, though it has a finite frequency at the transition and no pretransition (300) Bragg reflection is expected.

The variation of transition temperature with pressure is shown to be correlated to the sign of the tetragonality, and the observed dependence of T_m on pressure, alloying and T_c is in agreement with the theoretical predictions.

We have thus verified that a model of the A-15 structural transition based on a CDW mechanism with the Fermi surface lying close to the X point in the Brillouin zone is capable of explaining quantitatively the different phenomena associated with the transition.

A few of the predictions of the theory which may be put to test are the temperature dependence of the optic-mode frequency, the dependence of T_m and [110] transverse sound velocity above T_m in Nb_3Sn on uniaxial compressive stress, and the check of the observed correlation between sign of tetragonality and pressure dependence of T_m. On the theoretical side, a detailed investigation of the interplay between CDW and the BCS gap and the effects of T_m and T_c on one another, and a derivation of the Landau free energy used in the present calculation based on an actual 3D band structure are two areas in which work is clearly warranted.

ACKNOWLEDGMENT

One of us (R.N.B.) is grateful to the IBM Corporation for the grant of a fellowship.

*Supported in part by NSF Contract No. DMR75-20376.

[1]B. W. Batterman and C. S. Barrett, Phys. Rev. Lett. 13, 390 (1964); Phys. Rev. 149, 296 (1966).

[2](a) L. R. Testardi, T. B. Bateman, W. A. Reed, and V. G. Chirba, Phys. Rev. Lett. 15, 250 (1965); (b) L. R. Testardi and T. B. Bateman, Phys. Rev. 154, 402 (1967).

[3](a) G. Shirane and J. D. Axe, Phys. Rev. Lett. 26, 1803 (1971); Phys. Rev. B 4, 2957 (1971); (b) G. Shirane, J. D. Axe, and R. J. Birgeneau, Solid State Commun. 9, 397 (1971); (c) J. D. Axe and G. Shirane, Phys. Rev. B 8, 1965 (1973).

[4]M. Weger and I. B. Goldberg, in *Solid State Physics*, edited by H. Ehrenreich, F. Seitz, and D. Turnbull (Academic, New York, 1973), Vol. 28, p. 1.

[5]L. R. Testardi, in *Physical Acoustics*, edited by W. P. Mason and R. N. Thurston, (Academic, New York, 1973), Vol. X, p. 193.

[6]Yu. A. Izyumov and Z. Z. Kurmaev, Usp. Fiz. Nauk. 113, 193 (1974) [Sov. Phys.-Usp. 17, 356 (1974)].

[7]L. R. Testardi, Rev. Mod. Phys. 47, 637 (1975).

[8]P. W. Anderson and E. I. Blount, Phys. Rev. Lett. 14, 217 (1965).

[9]J. Labbe and J. J. Friedel, J. Phys. Radium 27, 708 (1966).

[10]R. W. Cohen, C. D. Cody, and J. J. Halloran, Phys. Rev. Lett. 19, 840 (1967).

[11](a) L. P. Gorkov, Zh. Eksp. Teor. Fiz. Pis'ma Red. 17, 525 (1973) [JETP Lett. 17, 379 (1973)]; Zh. Eksp. Teor. Fiz. 65, 1658 (1973) [Sov. Phys.-JETP 38, 830 (1974)]; (b) L. P. Gorkov and O. N. Dorokhov, J. Low Temp. Phys. 22, 1 (1976); Zh. Eksp. Teor. Fiz. Pis'ma Red. 21, 656 (1975) [JETP Lett. 21, 310 (1975)].

[12]B. M. Klein and J. L. Birman, Phys. Rev. Lett. 25, 1014 (1970).

[13]C. M. Varma, J. C. Phillips and S.-T. Chui, Phys. Rev. Lett. 33, 1223 (1974).

[14]L. F. Mattheiss, Phys. Rev. 138, A112 (1965); Phys. Rev. B 12, 2161 (1975).

[15](a) W. L. McMillan, Phys. Rev. B 12, 1187, 1197 (1975); (b) Ravindra N. Bhatt and W. L. McMillan, *ibid.* 12, 2042 (1975).

[16](a) L. J. Sham, Phys. Rev. Lett. 27, 1725 (1971); (b) J. Noolandi and L. J. Sham, Phys. Rev. B 8, 2468 (1973).

[17](a) J. R. Patel and B. W. Batterman, J. Appl. Phys. 37, 3447 (1966); (b) J. R. Patel and B. W. Batterman, Phys. Rev. 148, 662 (1966).

[18]W. Rehwald, M. Rayl, R. W. Cohen, and G. D. Cody, Phys. Rev. B 6, 363 (1972).

[19]L. J. Vieland, R. W. Cohen, and W. Rehwald, Phys. Rev. Lett. 26, 373 (1971).

[20]J. Perel, B. W. Batterman, and E. I. Blount, Phys. Rev. 166, 616 (1968).

[21](a) J. C. F. Brock, Solid State Commun. 7, 1789 (1969); (b) L. J. Vieland and A. W. Wicklund, Solid State Commun. 7, 37 (1969).

[22](a) C. W. Chu and L. R. Testardi, Phys. Rev. Lett. 32, 766 (1974); (b) C. W. Chu, *ibid.* 33, 1283 (1974).

[23]L. J. Vieland, J. Phys. Chem. Solids 31, 1449 (1970).

[24]L. R. Testardi, J. E. Kunzler, H. J. Levinson, J. P. Maita, and J. H. Wernick, Phys. Rev. B 3, 107 (1971).

[25]L. J. Vieland and A. W. Wicklund, Phys. Lett. A 34, 43 (1971).